1992

Metastable defects in hydrogenated amorphous silicon nitride

Elaheh Sigari
San Jose State University

Order Number 1350114

Metastable defects in hydrogenated amorphous silicon nitride

Sigari, Elaheh, M.S.

San Jose State University, 1992

U·M·I

300 N. Zeeb Rd.
Ann Arbor, MI 48106

Metastable Defects In
Hydrogenated Amorphous Silicon Nitride

A Thesis

Presented to

The Faculty of the Department of Physics

San Jose State University

In Partial Fulfillment

of the Requirements for the Degree

Master of Science

By

Elaheh Sigari

August, 1992

APPROVED FOR THE DEPARTMENT OF PHYSICS

Karamjeet Arya

Dr. Karamjeet Arya, Physics Dept. SJSU

Mark S. Crowder

Dr. Mark S. Crowder, IBM San Jose

Kumars Parvin

Dr. Kumars Parvin, Physics Dept. SJSU

APPROVED FOR THE UNIVERSITY

Serena N. Stanford

ABSTRACT

METASTABLE DEFECTS IN HYDROGENATED AMORPHOUS SILICON NITRIDE

by Elaheh Sigari

In this research project, it is reported that the light-induced paramagnetic defects in hydrogenated amorphous silicon nitride can be annihilated down to a saturation level by longer ultra-violet exposure at room temperature. The amount of annihilation will be much less when the hydrogenated thin film is exposed to UV-light at low temperature (77°K). These findings are in support of the passivating of light-induced defects by hydrogen during prolonged UV-exposure. However, the observed results can be also due to the charge motion which results in the production of new diamagnetic defects.

The thermally induced decay of the light induced paramagnetic defects follows a time dependence stretched exponential, $\exp[-(\frac{t}{\tau})^{\beta}]$. When annealing these defects at temperatures below 473 °K, β appears to be independent of annealing temperature. This result indicates that a tunneling or hopping mechanism is involved in the annealing process. However, annealing of light induced defects at temperatures above 473 °K displays a decrease in the β value. This result suggests that local structural changes occur during the annealing process.

Acknowledgements

Appreciation is extended to all those whose assistance and effort have made this study possible. I wish to thank IBM corporation for giving me the opportunity to use their equipment to work on this project. I wish to gratefully thank Dr. Mark Crowder for his encouragement, insightful recommendation, guidance and support throughout this study. I also wish to thank Dr. Arya and Dr. Parvin for their time, effort , and encouragement.

I also wish to thank Dr. John Baglin and Ms. Dolores Miller for their support which made it possible for me to write this thesis. Finally, I thank my husband and my daughter for their unfaltering confidence in my abilities, and their invaluable support that made this thesis possible.

Table of Contents

1. Introduction

Hydrogenated amorphous silicon nitride (a-SiN:H) is commonly used in the microelectronic industry as the gate dielectric in hydrogenated amorphous silicon thin film transistors [1.1] . In addition, this material is used as an active layer for recording and storing a charge in metal-nitride-oxide-semiconductor memory devices [1.2]. Amorphous-SiN:H films are used as diffusion barriers for impurities, and inhibit local oxidation [1.3]. Currently, a-SiN is the material of the choice for flat panel display technology.

The SiN used in devices is amorphous and generally contains hydrogen. Hydrogen in hydrogenated amorphous silicon nitride (a-SiN:H) passivates defects in the material and, consequently, it improves the optical and electrical properties of a-SiN:H thin film. In addition, the presence of hydrogen creates Si-H and Ni-H bonds which contributes in providing a long time of storage of information in the memory devices [1.4].

Essential to the understanding of the electrical properties of amorphous silicon nitride is the involvement of defect states [1.5]. These defects (Fig. 1.1) can act as charge trapping centers and greatly influence the properties of the SiN film [1.6]. The dominant defect in a-SiN:H responsible for

charge trapping is believed to be a threefold-coordinated Si dangling bond [1.7]. A fivefold-coordinated Si floating bond has also been proposed [1.8]. The dangling bond is amphoteric and can be found in three charge states (K^0, K^+, and K^-). The K^0 depicts the neutral dangling state and is paramagnetic (Fig. 1.1). Dangling bond states can also occur in two charge states: positively charged dangling bond denoted as K^+, and negatively charged dangling bond denoted as K^-. These states are energetically located between the valance (bonding) energy states and conduction (antibonding) energy states. The dangling bond states can undergo metastable changes due to charge trapping and charge recombination. These changes influence the optical and electrical properties of silicon nitride [1.9].

A number of studies have shown that the K^0-center density is increased during ultra -violet (UV) illumination [1.10]. The K^0 state defects can be photobleached by reillumination of SiN with photon energies in the range of 1.8 to 4.7 eV [1.11]. An electron spin resonance (ESR) study has shown that the photo- induced defects are metastable and can be annealed at relatively low temperature range (300 - 600 °K) [1.12].

Different models have been suggested for the production of the light induced K-centers. One model is involved with hydrogen motion, where two new dangling bonds will be created due to electron or hole recombi-

nation with the weak Si-Si bond. Then a hydrogen bond is diffused through created dangling bonds and prevents the recombination of them. Another model proposed for creation of K^0 centers can be due to the pre-exciting defect states, where the UV excitation will convert these positively and negatively charged sites into the paramagnetic K-centers. In this model the carrier transport can be provided by different processes. One process can be due to the tunneling of the carriers between two localized states which are very close to each other. This process is a non-energitical process and can happen fast. Another process for charge motion can be due to the transition of one electron from valance band to conduction band and consequently producing a free electron and hole that can be trapped by charge states in the gap and produce new K^0 centers. In this process, the excitation of a pair of electron and hole requires large energy. Therefore, in the range of small excitation energy an electron or hole can be sent to the charge states. Since the electron is more mobile compared to the hole, it is suggested that the created hole can be retrapped in its center but the electron will be sent to the defect sites.

The K^0 defects contain an unpaired electron, making them paramagnetic. ESR spectroscopy, which is also known as electron paramagnetic resonance (EPR), makes an accurate measurement of the density of these paramagnetic centers [1.13- 1.15].

Figure 1.1

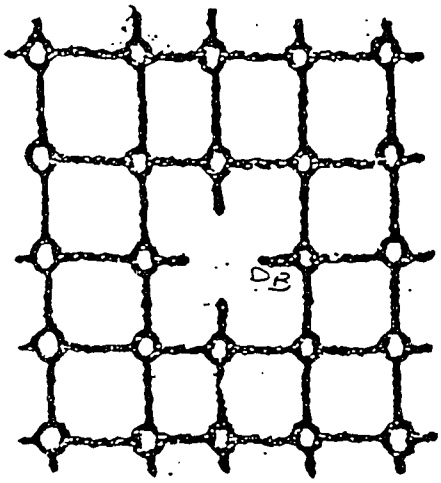

(a)

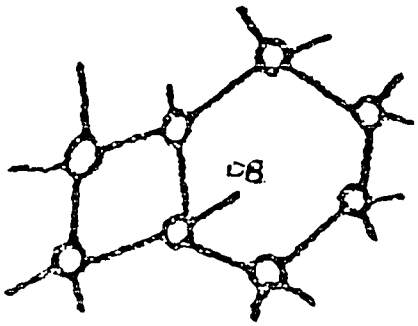

(b)

The ESR signal is indicative and proportional to the number of neutral defects. The K^+ and K^- centers are diamagnetic, and nondetectable by ESR spectroscopy. An ESR signal is produced by the interaction of microwave energy with paramagnetic centers. Application of microwave energy equal to the energy difference between the Zeeman-split energy levels induces quantum mechanical transitions between electron spin states, resulting in the net absorption of microwave energy. The ESR signal is due to this microwave absorption .

In our study we use electron spin resonance spectroscopy as a tool for monitoring the defect states in a-SiN:H [1.16,1.17]. ESR spectroscopy is uniquely used to quantify and identify the K^0 state. In this study ESR will be used to directly monitor the density of K^0 defects as a function of light condition and temperature.

The goal of this research project is to understand the mechanisms involved in the creating and depleting SiN defect states. The defect density is sensitive to illumination and undergoes changes due to the energy, time and flux of the light. The light-induced K^0 defect state is metastable and undergoes changes caused by heat (thermal annealing) and light energy. Photo-annihilation of the K^0 center, which is detected for the first time, is reported in this work. In this study, the annealing kinetics of the K^0 center is also determined. Analysis of annealing kinetics indicates tem-

perature dependent and temperature independent annealing properties. These results will be used to provide insight to the mechanism of annealing. This work is performed at IBM San Jose (Almaden Research Center and Storage Systems Products Divisions and in collaboration with Dr. Jerzy Kanicki at IBM Research Yorktown Heights Research Center), under the supervision of Dr. Mark Crowder.

2. Electron Spin Resonance

Electron spin resonance (ESR) is a form of spectroscopy used as a powerful tool to quantify and identify the paramagnetic defects in materials [2.1, 2.2, 2.3]. ESR can also be used to detect free radicals in solid, liquid, and gas, as well as to detect biradicals (two unpaired electrons). The resonance effect is due to quantum mechanical transition between electron spin energy states.

To observe ESR spectroscopy, an unpaired spin (paramagnetic) density is required. These unpaired spins may be due to electrons in the conduction band, valance band, or gap states.

Atoms with even numbers of electrons are spinless. Due to the Pauli exclusion principle, any two electrons sitting in the same state must have opposite spin numbers. This leads to a zero net magnetic dipole for each fully occupied electron state. The magnetic moment of an atom or ion in free space is given by:

$$\vec{\mu} = \gamma \hbar \vec{J} = -g\beta \vec{J} \tag{2.1}$$

where total angular momentum $\hbar\vec{J}$ is due to orbital angular momentum $\hbar\vec{L}$ and spin angular momentum $\hbar\vec{S}$. The factor g is defined by:

$$g = -\frac{\gamma\hbar}{\beta} \tag{2.2}$$

which different values of this factor distinguish one atom from another. For a free electron spin $g = 2.0023$, but generally deviates from this value due to orbital angular momentum contributions. The gyromagnetic ratio γ is defined as:

$$\gamma = \frac{\mu}{\hbar J} \tag{2.3}$$

β, the Bohr magneton, is equal to the spin magnetic moment of a free electron and is defined by $\frac{e\hbar}{2mc}$, where e and m are, respectively, the charge and mass of the electron. The magnetic moment will be:

$$\vec{\mu} = -g_e\beta_e\vec{S} \tag{2.4}$$

where $\vec{S}$ is the electron spin angular momentum ; g_e and β_e are, respectively, electron g and β factors. In the absence of external magnetic field, the electron spin energy levels are coincident. The presence of an external magnetic field influences the electron magnetic moment, and consequently splits the two degenerate electron spin energy levels. The energy of this interaction can be written as:

$$U = -\vec{\mu} \bullet \vec{H} = g\beta S H_z \tag{2.5}$$

where H represents the applied magnetic field in z direction.

For a free electron in space the energy difference between the two Zeeman-split electronic levels of the spin $\frac{1}{2}$ is given by:

$$U = \frac{1}{2} g\beta H - - (- \frac{1}{2}) g\beta H = g\beta H \tag{2.6}$$

Application of microwave energy ($\hbar v$) equal to the energy difference between two Zeeman-split levels induces a spin transition (Fig. 2.1). The ESR signal is due to net absorption. The resonance condition can be expressed by:

$$\hbar v = g\beta H \tag{2.7}$$

In the ESR measurement the resonance absorption is detected by sweeping the magnetic field (H) while keeping the microwave frequency (v) fixed . The spin Hamiltonian for the interaction of the atom with an external magnetic field can be written:

$$\mathcal{H} = \mathcal{H}_{ez} + \mathcal{H}_{nz} + \mathcal{H}_{hf} + \mathcal{H}_{s} \tag{2.8}$$

Figure 2.1

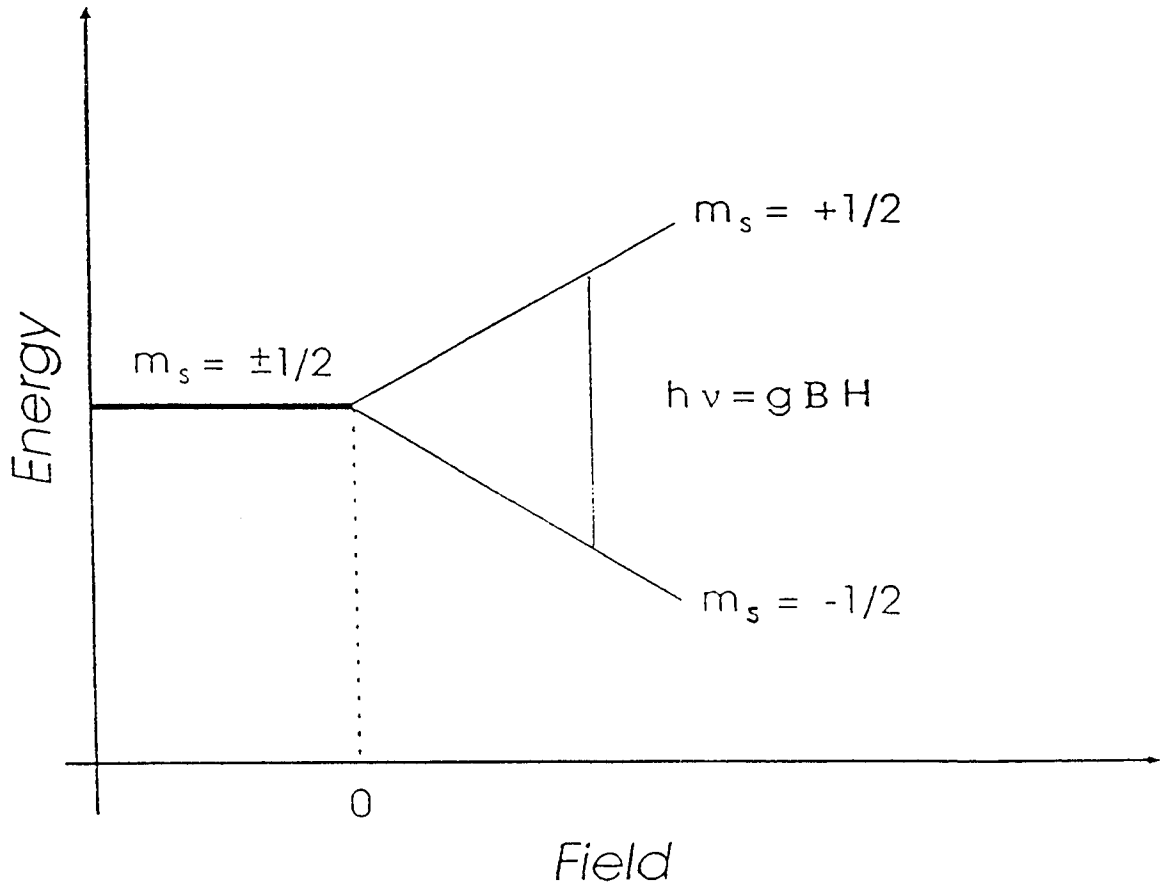

where:

$\mathcal{H}_{ez}$ = electronic Zeeman interaction

$\mathcal{H}_{nz}$ = nuclear Zeeman interaction

$\mathcal{H}_{hf}$ = nuclear hyperfine interaction

$\mathcal{H}_{s}$ = electron-coupled spin-spin interaction

The electron spin resonance signal is most often due to the electronic Zeeman interaction. The Hamiltonian for this interaction can be written as:

$$\mathcal{H}_{ez} = \beta_e \bullet \vec{S} \bullet g_e \bullet \vec{H} \tag{2.9}$$

The ESR signal will be influenced by other energy terms such as the hyperfine interaction and the electron-coupled spin-spin interaction. The Hamiltonian for this system can be written as:

$$\mathcal{H} = \beta_e \vec{S} \circ g_e \circ \vec{H} + \hbar \vec{S} \circ A \circ \vec{I} + B \circ \vec{S}_1 \circ \vec{S}_2 \tag{2.10}$$

where g, A, and B are (3 × 3) tensors, $\vec{S}$ and $\vec{I}$ are spin operators.

The hyperfine interaction is due to the interaction between the magnetic moment of an electron and the magnetic moment of a nucleus. The hyperfine interaction in the atom causes an additional splitting in the Zeeman electronic levels. The Hamiltonian for this interaction is:

$$H_{hf} = \vec{S} \bullet A \bullet \vec{I} \tag{2.11}$$

For a system with $S = \frac{1}{2}$, $I = 1$ the two electronic transitions have $\Delta m_I = 0$ (Fig. 2.2). Then the Hamiltonian will be:

$$\mathcal{H}_s = \mathcal{H}_{ez} + \mathcal{H}_{hf} \tag{2.12}$$

Equation 2.11 shows that the hyperfine interaction is independent of the external magnetic field, where the Zeeman interaction is dependent upon a magnetic field H (eq. 2.9). This distinction provides a method to distinguish between these two terms of the spin Hamiltonian.

Figure 2.2

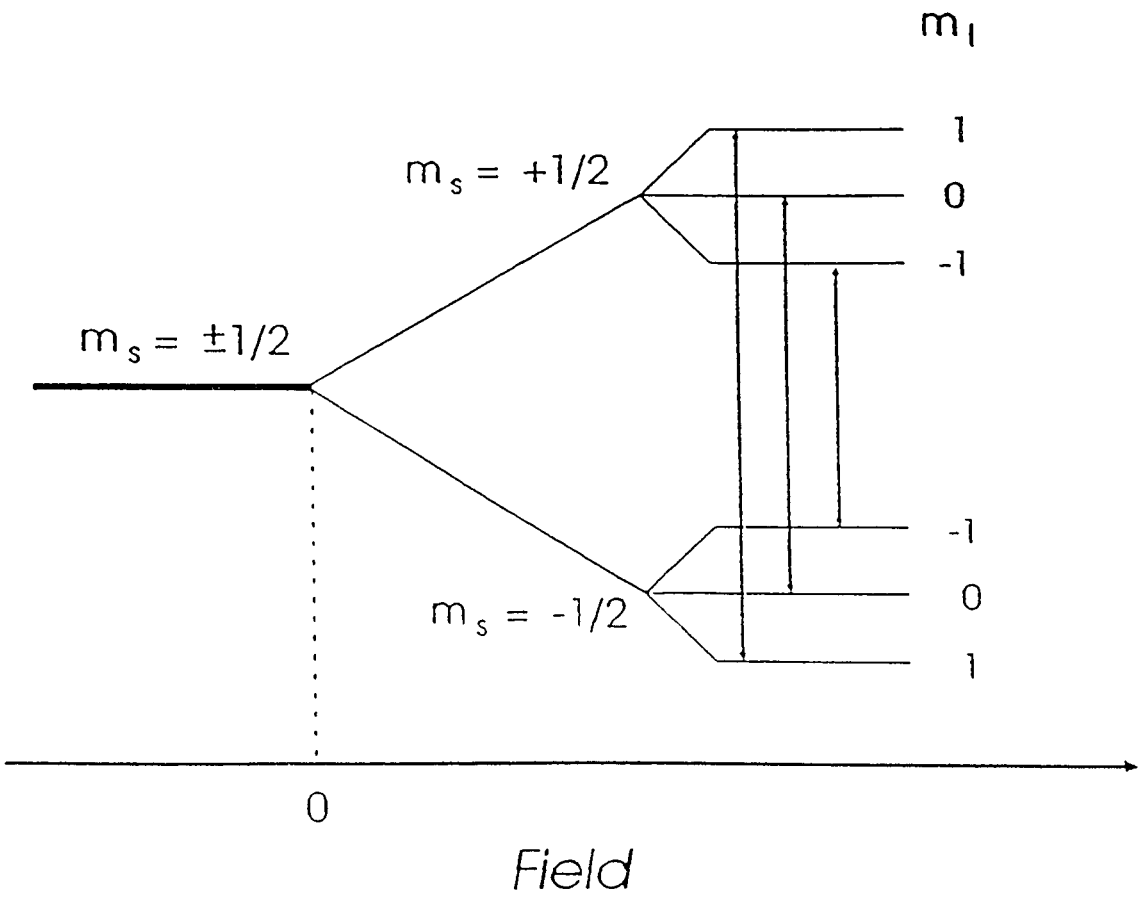

3. Amorphous Silicon Nitride

Amorphous silicon nitride (a-SiN) consists of covalently bonded atoms with a periodic ordering of atoms up to the third or forth nearest neighbors. Because of the short range atomic configuration, the electron states in this material cannot be described by well-defined $\vec{K}$ values. Amorphous-SiN films can be prepared by sputtering, chemical vapor deposition, evaporation or plasma decomposition of gases [3.1].

In an ideal amorphous-silicon nitride, each silicon atom has a fourfold-coordinated structure that can be covalently bonded to neighboring atoms. However, when a thin film of a-Si:N is produced, the restriction of the network prevents all atoms from having their perfect fourfold-coordinated structure. Consequently a threefold coordinated Si with an unpaired electron in a non-bonding orbital will be produced. Such an orbital is called a neutral dangling bond, denoted as K^0. Removal of an electron from the neutral dangling bond changes it to a positive dangling bond denoted as K^+, and the capture of an electron by K^0 will convert it to a negative dangling bond, K^-. Dangling bonds are known as the dominant defect centers in a-SiN:H [1.7].

3.1 Energy Gap

The main features of the energy band in the amorphous silicon nitride are similar to those in crystalline silicon nitrde. For example, there is a valance band and conduction band separated by an energy gap. However, there are some features that are different from crystalline form, such as the shape of the valance band and conduction band (Fig. 3.1). In amorphous semiconductors the valance- and conduction-band edges tail into the gap in a roughly exponential shape [3.1]. The magnitude of band tails depend on the sample preparation and also the stoichiometry of the material. In addition to the states located in the bands, there is a distribution of states throughout the gap. Anderson [3.1,3.2] has proposed that up to a certain energy level (mobile edge) the states are localized . The defect states located deep in the gap are localized states. Beyond the mobile edge the states are considered extended.

Cohen et al. [3.3] introduced a model for the energy states in which the tails extended into the gap and overlapped near the center of the gap with the Fermi level pinned at the overlap region. Now it is believed that the tails are not as extensive as in Cohen model and the pinning of the Fermi level is associated with defect states. These defect states are due to Si dangling bonds.

Figure 3.1

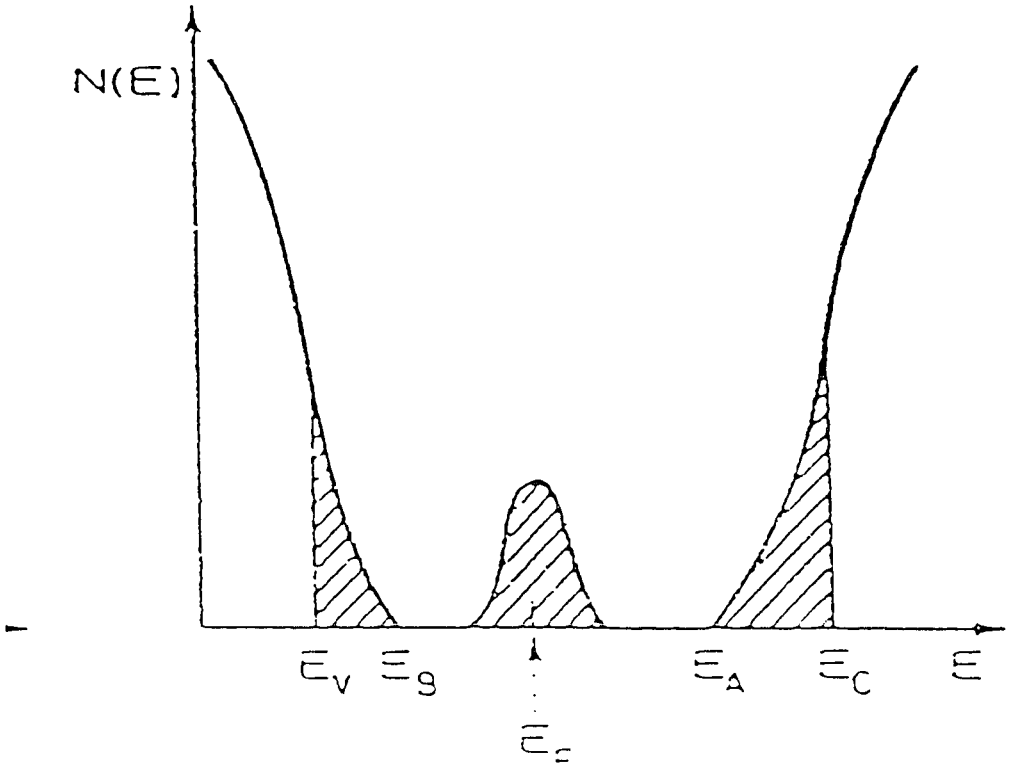

The electron energy levels of the dangling bonds are located in the mobility gap between the bonding (valance) states and antibonding (conduction) states. These dangling bonds contribute effectively to optical and electrical properties of a-Si thin films [1.5] and act as dominant recombination centers for excess electrons and holes, which results in lowering the conductivity of a-SiN thin films [1.7].

In addition to defect states, the states located in the band tails also contribute in a-SiN thin film properties. These states are due to exceptional configurations such as deviations of bond angles or lengths. For example, strained Si-Si weak bonds which have a large variety of bond length and bond angles from the Si-Si bonds in crystalline Si, results in localized states in the band tails.

Addition of hydrogen to a-SiN can affect the band tail states [3.4,3.5]. The hydrogenation of silicon-rich a-SiN changes Si-Si weak bonds, with bonding energy about 2.33 eV, into Si-H bonds with bonding energy of about 3.30 eV, which lie deeper in the valance band. This transition will increase the gap energy. However, in nitrogen-rich a-SiN the hydrogenation replaces Si-N bonds with Si-H nd N-H bonds [3.6]. The average energy of Si-N bonding is about 3.43 eV, while the energy for a N-H bond varies from 3.3 to 4 eV [1.4]. Therefore, hydrogenation of the nitrogen-rich a-SiN has less of an effect on the gap energy.

3.2 Correlation Energy

To determine the electronic structure of the amorphous semiconductors, different methods of measurement such as luminescence [3.7] and electron spin resonance [3.8] have been performed. But the energy position of the defect levels are still unknown. Anderson has proposed that amorphous semiconductors have a tendency to have paired electrons in the same bonding configuration [3.1], where the Coulomb interaction between electrons at the same site is nullified by energy due to electron-phonon interaction.

Anderson has also proposed that the localized states in the gap can either be doubly occupied or empty. This invokes a negative correlation energy for the amorphous-semiconductor, with K^0 at a higher energy level than K^-. The relaxation of K^0 centers to K^+ and K^- results in an decrease in the density of K^0 centers. Fig. 3.2 shows the energy levels in the gap of a negative correlation system containing K^+ , K^- , and K^0 defects. Addition of an electron from the valance band into the K^+ state, which results in the K^0 state, requires an energy like E_1. The addition of an electron from valance band into the K^0 state results in the K^- state and requires an energy like E_2. Thus, we can write:

$$K^+ + e(vb) + E_1 \rightarrow K^0 \qquad (3.1)$$

$$K^0 + e(vb) + E_2 \rightarrow K^-$$

Therefore we can write:

$$2K^0 \rightarrow K^+ + K^- + (E_1 - E_2) \qquad (3.2)$$

where for negative correlation energy $E_1 > E_2$.

However, some studies performed on the defect states in the amorphous semiconductors are based on the positive correlation energy [3.9, 3.10], where the K^- and K^+ states lie at a higher energy level in the band gap than the K^0 state.

Figure 3.2

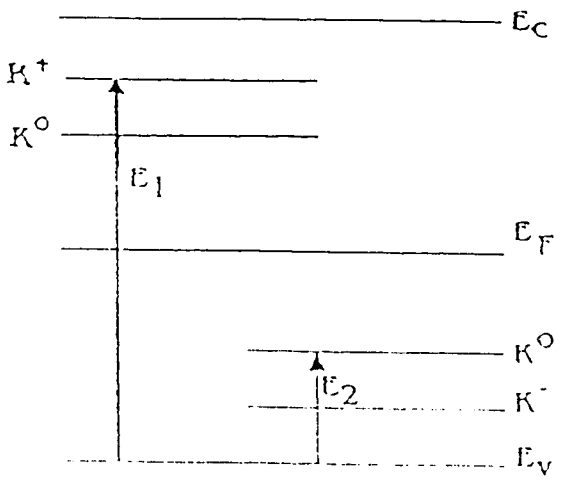

3.3. Light Induced Defects in Hydrogenated Amorphous Silicon Nitride

Several studies have been reported to show the effect of ultra-violet light illumination on the density of the neutral charged defects [3.11-3.13]. K^0 centers are created and photobleached in a-SiN :H films by light illumination [3.11-3.15]. To explain the creation of neutral charged defects, different models have been proposed.

Staebler-Wronski proposed that for a-Si upon light exposure, the photo-excited electron-hole pair recombine at the site of Si-Si weak bond and result in the lowering of the weak bond energy, consequently breaking the bond and creating two dangling bonds. The motion of hydrogen in between these bonds prevents the rejoining them [1.10,2.16]. In this model new defect centers are created by light illumination.

Alder suggested another model [3.17] which includes the hypothesis that the creation of the neutral charged defects produced by light is caused by changing the pre-existing states (K^-, K^+) into K^0 centers by trapping electrons or holes. Therefore, the total number of defects remain constent and no new defects are produced by light. The Alder model and other

charge transport models are consistent with both positive and negative correlation energy .

Figure 3.3 shows two level energy states which are ground state (K^-, K^+) and excited state (K^0). Due to light illumination, when the photon energy is equal to E_1, a transition from ground state to excited state will happen . However, to make a transition from excited to ground state an energy equal to E_2 is required.

To thermally anneal the excited state, K^0 , an activation energy (E_a) barrier, must be overcome. Alternatively, the transition probability may be influenced by quantum mechanical tunneling from the excited state to ground state.

In the following chapter the effect of UV light illumination on the density of neutral charged defects will be shown. Electron spin resonance is used to quantify and identify the K^0 centers, where the ESR signal is proportional to the number of neutral charged defects. The rate of change of the density of K^0 centers will be determined as a function of illumination time. It will be shown that light induced metastable defects can be annihilated by further UV-illumination at room temperature. The influence of the low temperature (77° K) illumination on annihilation will be determined.

Figure 3.3

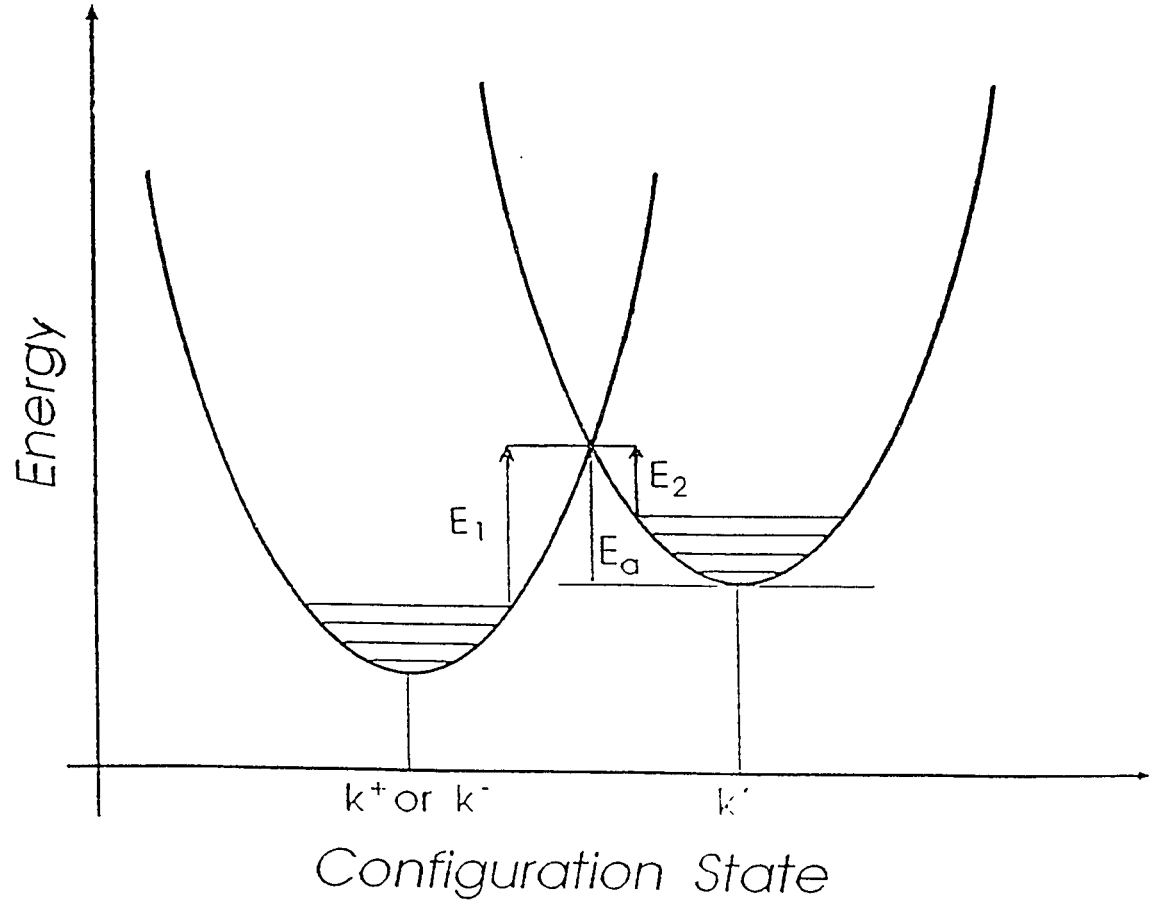

3.4 Experimental Methods

The samples used for these experiments are hydrogenated, amorphous silicon nitride thin films which are of device quality and are prepared by Dr. Jerzy Kanicki at IBM Research, Yorktown Heights. These samples are made by plasma enhanced chemical vapor deposition using silane (SiH_4) and ammonia (NH_3) gas mixtures and are deposited to a thickness of 1300 nm onto a fused quartz substrate held at 250 ° C. The nitrogen to silicon atomic ratio in these films is 1.6 and contains 38% atomic hydrogen.

The ESR measurements were performed on a Bruker Instruments ER-200 and an ESP-300 spectrometer using X-Band microwave frequency (9.7 GHZ) with a non-saturating microwave power of 2.0 mW and 5 Gauss (100 KHZ) magnetic field modulation. The ESR spectra were taken at room temperature and at 77°K and were highly reproducible (~ 4% error). The samples used for the ESR study were 5-7 strips (2mm X 4mm). For the ESR measurement the samples were placed in the quartz sample tube and aligned perpendicular to the external magnetic field. Spin concentrations were measured by a comparison with a ruby standard supplied by National Bureau of Standards.

Illumination of samples was provided by using an IR filtered, 500 Watt Oriel Xenon Ultra-Violet lamp with the photon energy up to about 5.5 eV (180 nm). When the samples were illuminated at room temperature a flow of cool nitrogen was applied to the samples to prevent overheating during illumination. The power of the light used for illumination of samples was measured by an Optical Associates INC.1 306 U.V. power meter located near the sample.

Amorphous SiN deposited at 250 ° C contains K^0 ESR centers prior to UV illumination. This ESR signal, which is most likely produced during film preparation, represents the "as deposited" K^0 spin density. Typically, this signal intensity is 10-20% of the light induced ESR signal (LESR) intensity. This ESR signal can be annealed (see chap. 5.1) and has the same g-value and linewidth as the LESR signal (Fig. 3.4). In most of our studies the "as deposited" signal represents the dark ESR (DESR) signal. However, prior to some of our annealing studies the "as deposited" sample is preannealed and the resultant ESR signal is considered as DESR signal.

The SiN films are illuminated out of the ESR microwave cavity and placed in the cavity for the ESR measurements. Care was taken to align the sample in the cavity, and the ESR signal reproducibility was better than ±4%. To obtain the light induced ESR signal (LESR), the "as de-

posited" ESR signal is subtracted from the signal recorded after light illumination. Illumination in the cavity showed no significant decay in the ESR signal upon cessation of the UV lamp (i.e., no rapid component after light is turned off).

For the high temperature and low temperature studies, the samples were sealed in evacuated quartz EPR sample tubes backfilled with 4mm Hg of helium gas. Annealing of the samples in the range of 373 to 523°K was conducted, out of the ESR cavity. A Bruker ER4114-HT high temperature heater was used to anneal the samples. The sample temperature was monitored by a RhFe high-temperature calibrated thermocouple placed near the sample.

However, annealing of the subject sample at room temperature was performed in the same cavity that the spectrum was taken and it was not removed out of the cavity during the annealing process. In this study the temperature of the subject sample was not monitored by the thermocouple.

Figure 3.4

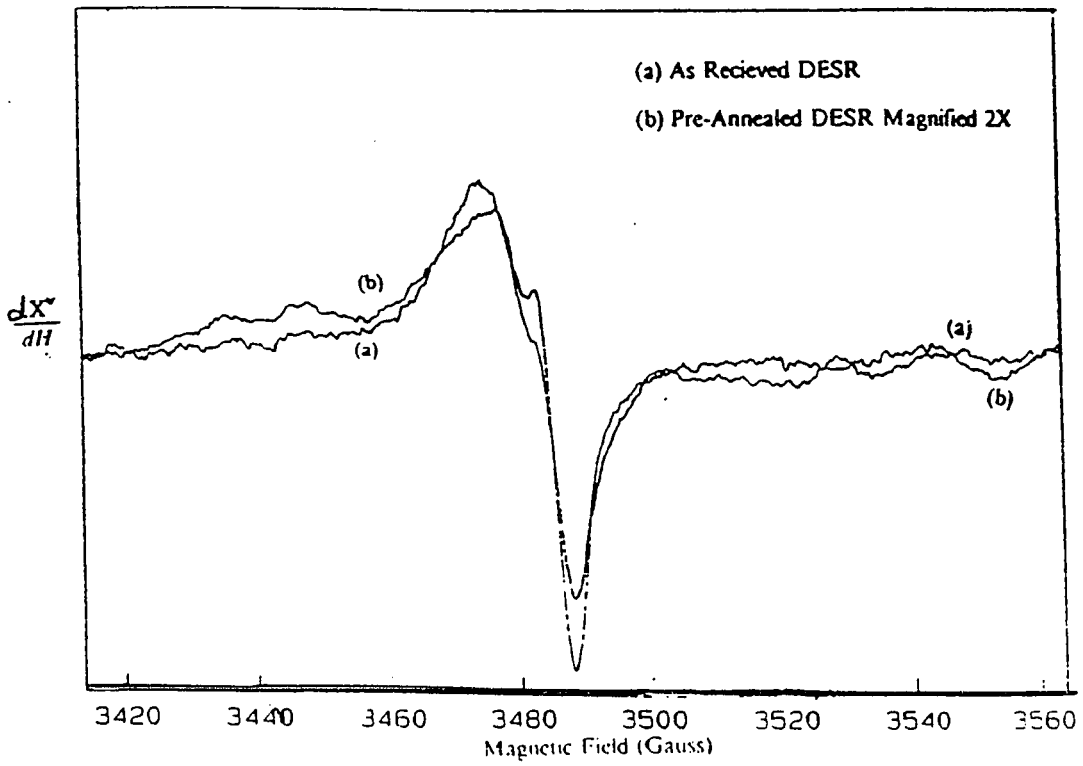
(a) As Recieved DESR
(b) Pre-Annealed DESR Magnified 2X
dX''/dH
(b)
(a)
(aj
(b)
3420
3440
3460
3480
3500
3520
3540
3560
Magnetic Field (Gauss)

4. Annihilation Of Light Induced Metastable Defects In a-SiN

Several studies have shown that under UV light illumination, the number of neutral charged defects in the a-SiN:H films will increase [1.10]. In this chapter, it is shown that when a-SiN·H is illuminated by UV light at room temperature, the number of K^0 centers will slowly increase to a maximum level which upon further UV illumination will slowly decrease. The observed decay after saturation in the density of the neutral defects is denoted as annihilation. The effect of light on annihilation in a-SiN film at low temperature (77°K) is determined. A mechanism to explain the annihilation is suggested.

4.1 Result

The SiN film is illuminated at room temperature with UV light for varying period of time and after each period of illumination an ESR signal from the sample at room temperature is recorded. The sample is not exposed to UV-light during the detection of the ESR signal, and it is known that no significant change, due to the annealing at room temperature, will occur while the ESR signal is recorded (see chap.5). To obtain the light induced ESR signal (LESR), the as deposited ESR signal

is subtracted from each of the signals recorded after each period of light illumination. A time dependent increase followed by a decrease of the LESR signal in a-SiN:H is observed during the UV illumination. Fig. 4.1 shows the K^0 center density changes versus UV-illumination time. First, due to the UV-illumination, K^0 centers are activated and after 2 minutes the density of these states is maximized. Then, when the sample is exposed to UV light for another 2 minutes, no change in the concentration of LESR is observed. However, exposing the sample to longer UV- exposure causes the K^0 center to irreversibly decay (annihilation). UV exposure is carried out for 240 minutes, and about 82% of light induced K-centers are extinguished. The light illumination is continued for 1101 minutes, and no further decay in the LESR signal is detected. Therefore, annihilation is maximized and an LESR signal is left (18%).

After one day at the room temperature, without UV-illumination, further decay in the LESR signal is observed, and after 5 days at room temperature, it is found that all of LESR is completely extinguished. The decay after full annihilation is due to a thermally induced decay (annealing). Thus, some K^0 centers which can not be annihilated can be annealed (see chap. 5 for room temperature annealing of K^0).

Figure 4.1

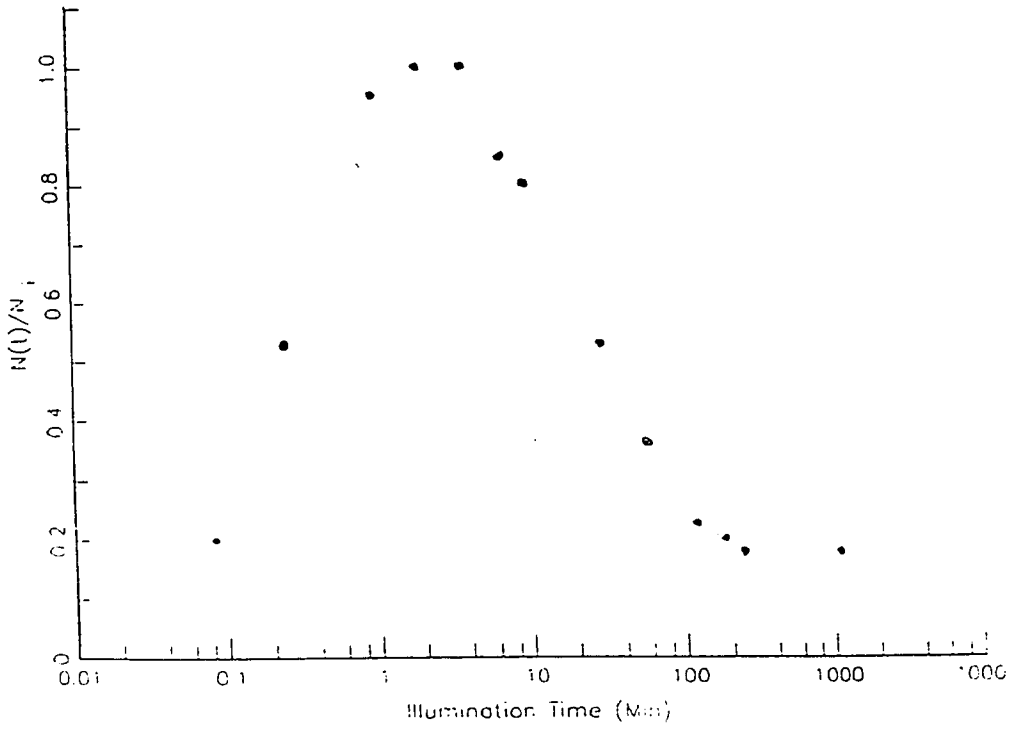

A change in the linewidth of the LESR signal is observed due to annihilation. As shown in Fig. 4.2, by increasing the UV-illumination time, the LESR signals begin to broaden. However, no change in the g value of the LESR during the illumination is detected (g = 2.003). Fig. 4.3 shows the trace of the ESR signal when the SiN film is illuminated for different time intervals.

The "as deposited" signal measured for a-SiN:H samples prepared at 250 ° C, is a considerably larger signal (~20% of LESR signal) which is indicative of the high density of pre-existing neutral charged defects. To obtain a DESR signal the "as deposited" sample is preannealed for about 20 hours at 250 ° C. This treatment completely anneals the K^0 centers which were induced due to the film preparation, and the remaining signal represents the background ESR signal. When the preannealing process was repeated for other studies, it was found that only 300 minutes annealing at 250 ° C is sufficient to achieve to the same ESR density. This sample was exposed to UV-light and the density of the K^0 centers was measured at different time intervals. The change in the K^0 centers as a function of time is shown in Fig. 4.4.

Figure 4.2

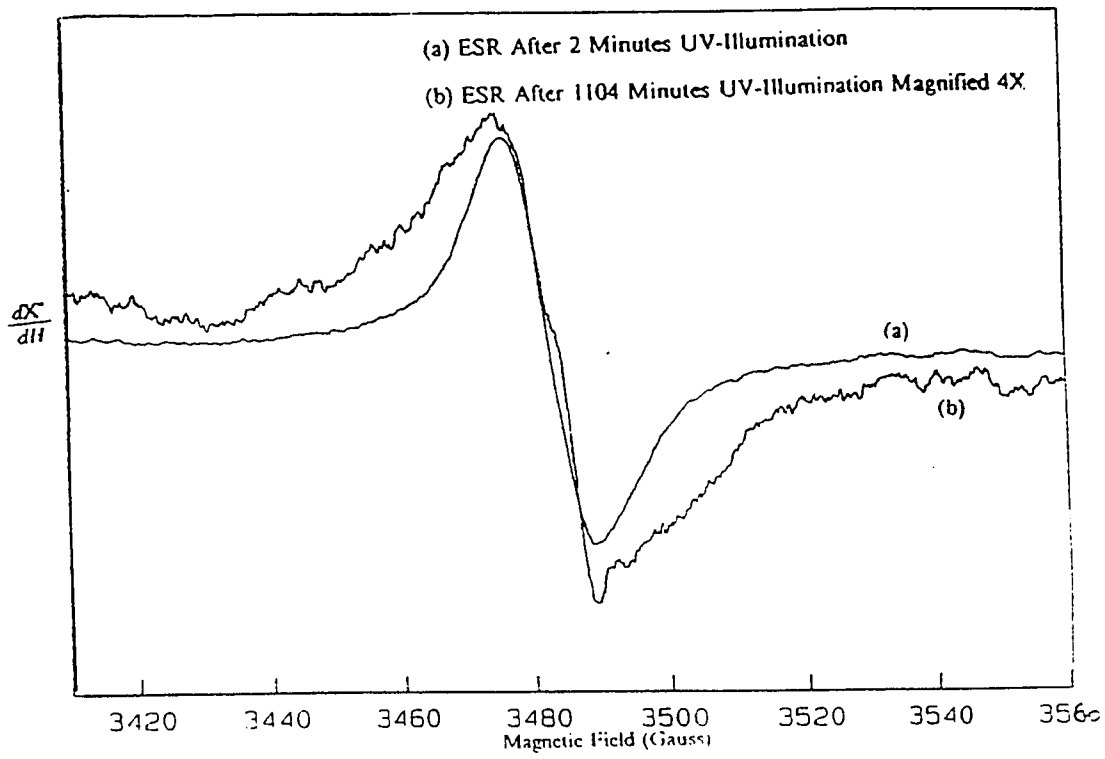
(a) ESR After 2 Minutes UV-Illumination
(b) ESR After 1104 Minutes UV-Illumination Magnified 4X
dX/dH
(a)
(b)
3420
3440
3460
3480
3500
3520
3540
Magnetic Field (Gauss)

Figure 4.3

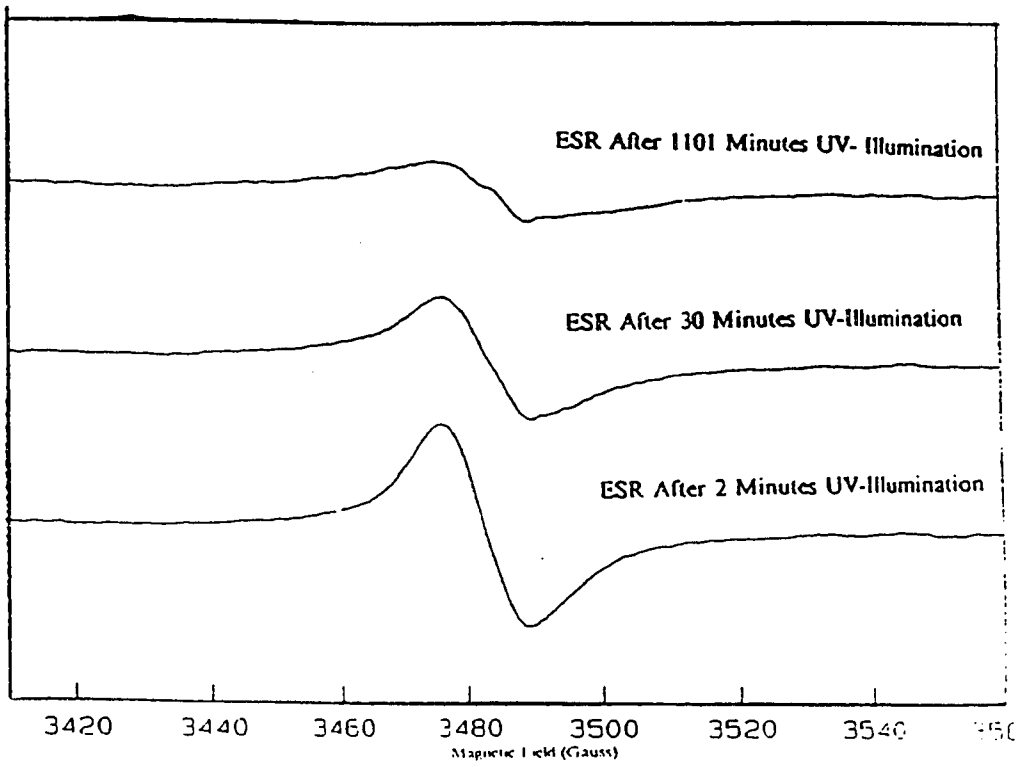
ESR After 1101 Minutes UV- Illumination
ESR After 30 Minutes UV-Illumination
ESR After 2 Minutes UV-Illumination
3420
3440
3460
3480
3500
3520
3540

Figure 4.4

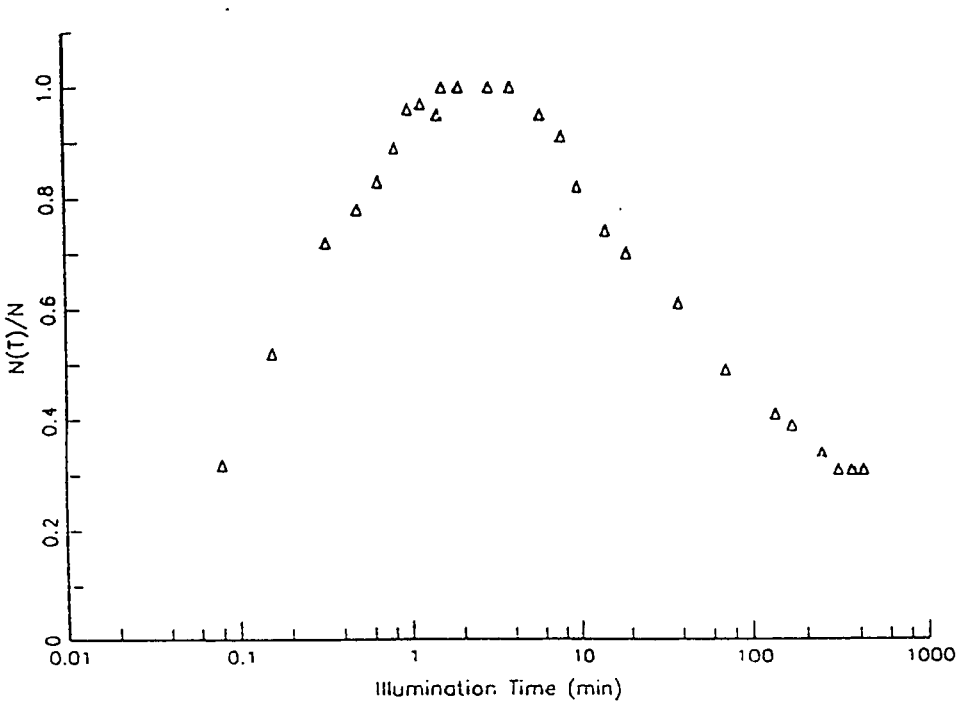

To characterize annihilation, another experiment was performed at 77°K. In this experiment the sample is preannealed at 250 °C for 1010 minutes and a signal from the sample is recorded at room temperature (DESR). It is found that 48% of the neutral defects present in the "as deposited" sample are preannealed. Then the sample was illuminated for different period of time at 77°K and an ESR signal for each period is also recorded at 77°K. In this experiment the sample, located in the quartz tube, was illuminated inside a quartz dewar which is filled with liquid nitrogen. Then the sample is transferred to the ESR cavity while it is kept in 77°K and an ESR signal is recorded. In this study a continuous increase in the light induced ESR is observed and no decrease in LESR signal could be detected. This result can be due to the contribution of the ESR signal generated by sample tube and dewar. As it was mentioned, the sample tube and dewar both are made of quartz, which can have significant ESR signals at low temperature. These signals can grow as the tube and dewar are illuminated at low temperature. Therefore, it is possible that the continuous increase observed in the LESR signal is in fact due to the sample tube or dewar. In this way, if there is a decrease in the LESR from the sample, it is possible that this decrease can not be detected because of the large signal generated by sample tube and dewar.

To determine the annihilation more accurately, another study in the 77°K was performed. This time, the preannealed a-SiN film was illuminated with UV light at 77°K for different periods of time and each time a signal at room temperature was recorded. The signal due to the quartz decays quickly at room temperature. Therefore, in this study the signal caused by quartz will not affect in our results. To obtain the light induced signal (LESR), the DESR is subtracted from each of the signals recorded after each period of light illumination. For the first 10 minutes of UV illumination at 77°K, an increase in the LESR is observed. However, when the sample is illuminated for 10 more minutes, no change in the density of the defects is observed (saturation level). UV illumination of the sample at 77°K for longer than 20 minutes causes decay in the LESR density, where after 100 minutes of UV illumination at 77°K about 33% of LESR will be decayed. Further, UV illumination of the sample at 77°K is carried out for another 30 minutes and no further decay in the density of K^0 defects is observed .

The sample illuminated at 77°K is then re-illuminated at room temperature. A time dependent decay in the LESR due to the UV illumination at room temperature is observed. A total decay of 67% of the maximum LESR signal is detected after 34 minutes of room temperature illumination. When the light illumination is carried out for another 120 minutes on the sample, no further decay in the LESR is observed. The decay

of 67% is very similar to the decay observed at the first set of studies of UV-illumination at room temperature (Fig. 4.4).

To detect the reversibility of the annihilation, this sample is further exposed to UV light at 77°K. This study shows that after 16 minutes of UV illumination at 77°K, 25% of the annihilated LESR at room temperature can be reproduced. When this sample is illuminated for more than 16 minutes no change in the density of the LESR is observed. Fig. 4.5 shows the change in the K^0 centers in the sample, due to the UV illumination at room temperature and UV illumination at 77°K.

Figure 4.5

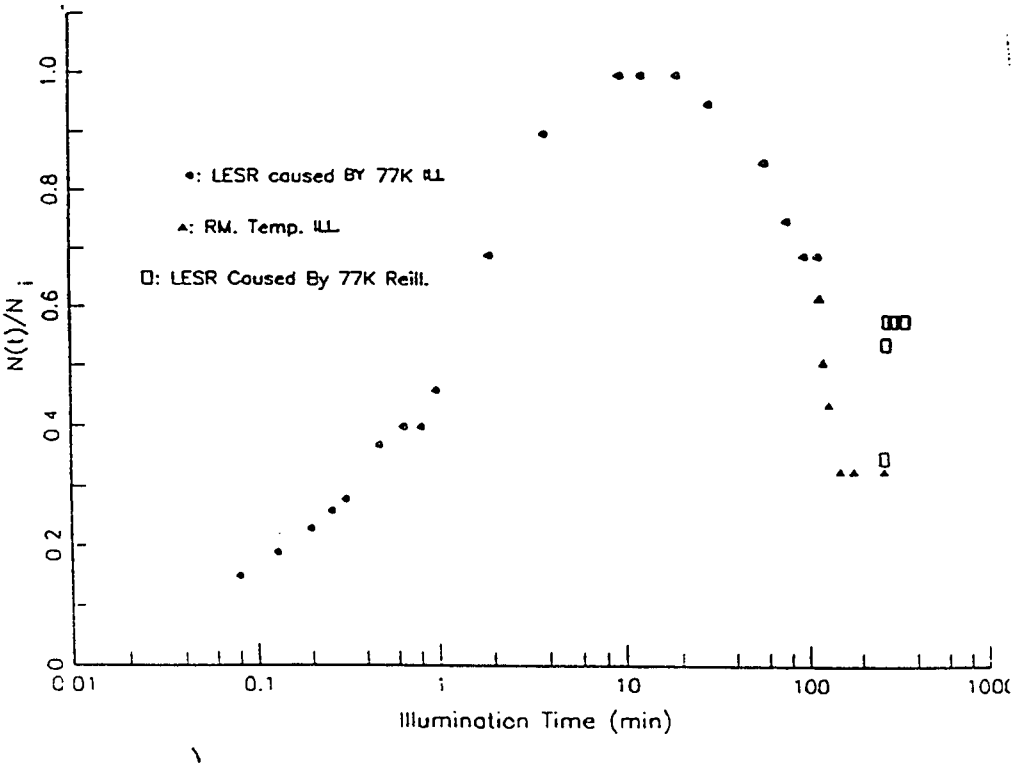
•: LESR caused BY 77K ILL
▲: RM. Temp. ILL
□: LESR Caused By 77K Reill.
N(t)/N i
0
0.2
0.4
0.6
0.8
1.0
0.01
0.1
1
10
100
Illumination Time (min)

4.2 Discussion

Films deposited at 250° C and 400° C are both prepared by PECVD but with different hydrogen concentration, 38 atomic % and 31 atomic %, respectively. Since we find more hydrogen in SiN films deposited at 250 ° C, we suggest that irreversible decay caused by UV-illumination in these films is due to hydrogen concentration and the model proposed for annihilation process can involve the motion of a hydrogen bond. Kanicki et al. [4.1] have performed IR studies on annihilated samples and have shown that, after annihilating the sample by UV-exposure, the concentration of N-H bond decreases while an increase in the concentration of Si-H bond is observed. A possible mechanism for the annihilation of the LESR signal is through the rearrangement of the bond configuration and consequently breaking N-H bonds where the produced hydrogen bonds can diffuse through the sample and passivate the light induced silicon dangling bonds.

$$N - H + h\nu \rightarrow N^{\bullet} + H^{\bullet} \tag{4.1}$$

$$Si^{\bullet} + H^{\bullet} \rightarrow Si - H$$

$$Si^{\bullet} + N^{\bullet} \rightarrow Si - N$$

Another possible mechanism due to the configuration rearrangement is breaking the H-H bond and the diffusion of hydrogen through the sample and passivating the silicon dangling bond. In this case we will have:

$$N - H \rightarrow N^{\bullet} + H^{\bullet} \qquad (4.2)$$

$$H - H \rightarrow H^{\bullet} + H^{\bullet}$$

$$Si - Si \rightarrow Si^{\bullet} + Si^{\bullet}$$

$$Si^{\bullet} + H^{\bullet} \rightarrow Si - H$$

$$Si^{\bullet} + N^{\bullet} \rightarrow Si - N$$

Good evidence for the contribution of hydrogen in the annihilation process is our study which was performed at low temperature. According to this study a small amount of annihilation ($\sim$ 28%) is observed at low temperature, which is consistent with a small hydrogen diffusion coefficient at low temperature. Therefore, when a N-H or H-H bond is broken at low temperature, the hydrogen bond cannot travel far and consequently the broken bonds recombine quickly. This way only a small amount of the K-centers present in the area can be passivated by the hydrogen, which results in a small decay of LESR. In this study after UV-exposure of the sample at low temperature, the LESR signal is recorded at room temperature. Therefore, there will be hydrogen diffusion through the

sample, which passivates some of the light induced defects and consequently generates a small decrease in the LESR signal.

In support of this model is the broadening of the ESR signal during the annihilation. This broadening is caused by hyperfine interactions between the magnetic moment of the unpaired electron of the silicon with the magnetic moment of the hydrogen nucleus (Fig 4.2).

However, we should consider the possibility of annihilation of K^0 centers due to the charge motion. In this model the photo-excited electrons and holes are trapped by the deep K^0 centers and consequently other stable charge trapping centers are generated which are diamagnetic and are not detectable by ESR. This model is consistent with the electrical stress measurement performed on the annihilated SiN films. According to this measurement, even though a large number of the K^0 centers are annihilated the number of the trap centers remain almost unaffected. We can conclude from this result that, in the UV-illuminated SiN films, the K^0 centers are not the only trapping centers for the carriers but also the charge states contribute as the trap centers. However, due to the previous studies it was believed that K^0 centers are the only trap centers for the carriers in the UV-illuminated SiN films.

Finally, in the last part of our study we find that some of the K^0 centers that were annihilated at room temperature can be reproduced (~28%) by further UV exposure of the sample at 77 °K. This result can be caused by local configuration rearrangement, such as that due to light illumination. Si-H bonds will be broken and the created hydrogen will recombine with the local nitrogen bond and result a silicon dangling bond.

Another model can be suggested for the reproduction of LESR at low temperature. In this model we propose that the production of the LESR is taking place at the same time that the annihilation is observed. But the rate of the production of the defects at room temperature is so small compared to the annihilation of them that we cannot observe it. However, when we continue the experiment at low temperature, since the rate of the hydrogen diffusion is very small at low temperature, then the amount of the production of the light-induced defects is more significant.

5.Thermal Annealing Of Light Induced Metastable Defects in a-SiN

To understand the mechanisms responsible for the creation and depletion of metastable light-induced defects, several studies on the annealing kinetic of a-SiN:H have been reported [5.1-5.2]. Investigation of a-SiN:H films shows that dangling bonds created by illumination can be annealed [5.3]. It has also been shown [5.4] that the annealing of the light-induced defects is described by a time dependence stretched exponential decay:

$$exp[-(\frac{t}{\tau})^{\beta}] \qquad (5.1)$$

where $0 < \beta < 1$. For small departures (Δ) from equilibrium, the decay is given by : $\frac{d\Delta}{dt} = -\nu\Delta$. The relaxation rate ν shows a power law time dependence, $\nu \simeq t^{-\alpha}$, where $\alpha < 1$.

Due to eq(5.1), there is a dispersive transport in the a-SiN indicative of an exponential energy distribution of traps [$\exp(\frac{-E_a}{KT_0})$] where KT_0 exhibits the width of the distribution. The dispersion parameter α is given by $1-\alpha = \beta = \frac{T}{T_0}$. The relaxation time τ in eq (5.1) is thermally activated and is described by $\tau = \tau_0 \exp[\frac{E_a}{KT}]$, where τ_0 is the pre-exponential coefficient, E_a is the activation energy, and K is the Boltzmann 's constant. The studies on a-SiN:H films prepared at 400 °

C have shown a temperature dependent β and τ [2.11]. In this section, the thermal annealing of the metastable light-induced defects in a-SiN:H films prepared at 250 ° C will be investigated. A mechanism responsible for the annealing process will be suggested.

5.1 Results

To determine the initial defect signal present in the a-SiN:H film, prior to annealing or illumination, an ESR signal from each sample is taken. This signal represents the "as deposited" ESR signal intensity. This ESR signal represents the dark ESR (DESR) signal with additional K^0 spin density, which is most likely produced during film preparation. The true DESR is obtained by preannealing the "as deposited" sample (prior to-UV exposure). Preannealing the sample at 523° K for 360 minutes results in a 60% decay of K^0 defects and represents the true DESR signal used for the analysis of the annealing data. The ESR signals taken from a "as deposited" sample and a preannealed sample are shown in Fig. 2.4. The samples are illuminated at room temperature using a UV lamp for about 2 minutes until maximum paramagnetic defect density is created (see annihilation chap. 4). This signal is used as a reference point from which we can cycle the samples through a series of annealing and reillumination processes. From the maximum ESR illuminated state (2 minutes UV illumination, see Fig 4.1), the sample is isothermally annealed. Isothermal annealing experiments were performed below sample deposition temperature over a range of temperature from 300°K to 573°K for varying periods of time.

After each period of annealing, to expedite cooling process, the samples are immersed in room temperature water. The ESR spectrum is recorded at room temperature after each period of annealing. The annealing process produces a decrease in the linewidth of the LESR signals (Fig. 5.1.2). Throughout annealing and recording ESR signals the samples are not exposed to Ultra-Violet light. To obtain the light-induced ESR signals (LESR), the DESR spectrum is subtracted from each of the illuminated and annealed signals. A time dependent decay of the LESR signal in a-SiN:H is observed during isothermal annealing . A stretched exponential function (eq. 5.2) was used to best fit the isothermal annealing curves:

$$\frac{N(t)}{N_0} = A \exp\{-(\frac{t}{\tau})^{\beta}\} + (1 - A) \qquad (5.2)$$

where N(t) is the density of the light induced defects at the annealing time t, N_0 is the density of the defects before annealing (t = 0). The parameters A, β, and τ are found by curve fitting in eq. 5.2 with the data.

A represents the maximum percentage of defects that can be annealed, which is a function of annealing temperature (A = 1 represents 100% annealing of the LESR signal). The parameter τ follows the Arrhenius relation:

$$\tau = \tau_0 \exp\left(\frac{E_a}{KT_A}\right) \tag{5.3}$$

where τ_0 is the exponential pre-factor, E_a is the apparent activation energy, and K is Boltzman's constant.

Figure 5.1

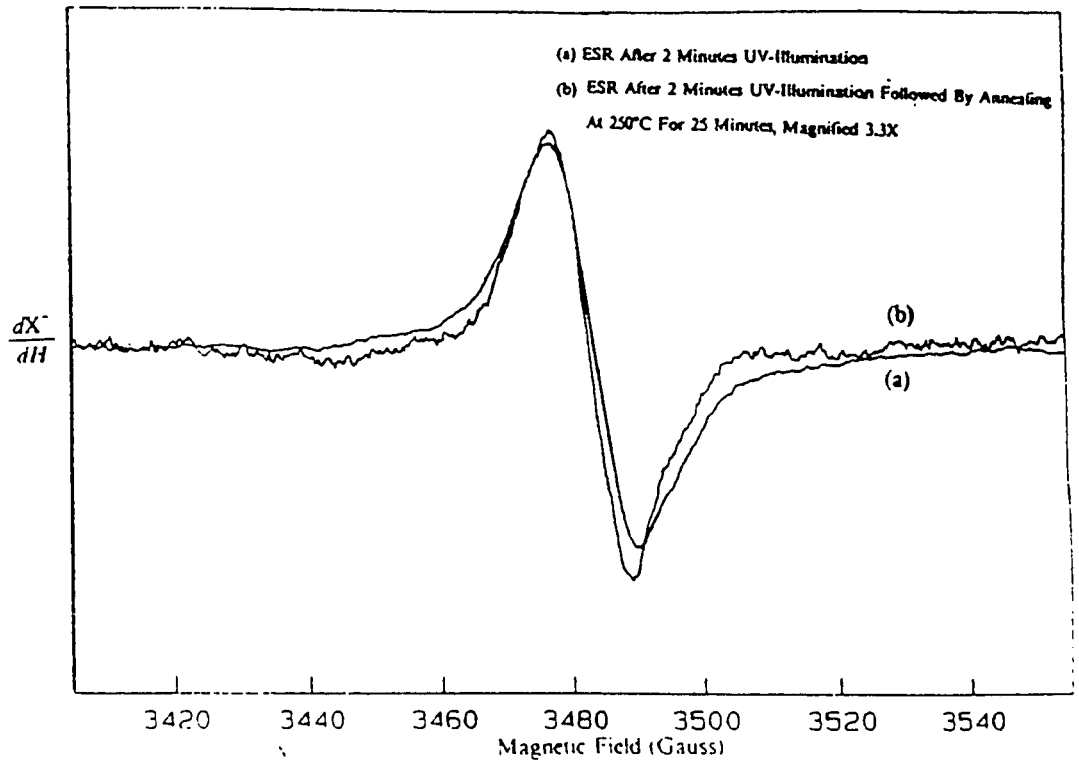
(a) ESR After 2 Minutes UV-Illumination
(b) ESR After 2 Minutes UV-Illumination Followed By Annealing At 250°C For 25 Minutes, Magnified 3.3X
dX/dH
(b)
(a)
3420
3440
3460
3480
3500
3520
3540
Magnetic Field (Gauss)

Figure 5.2

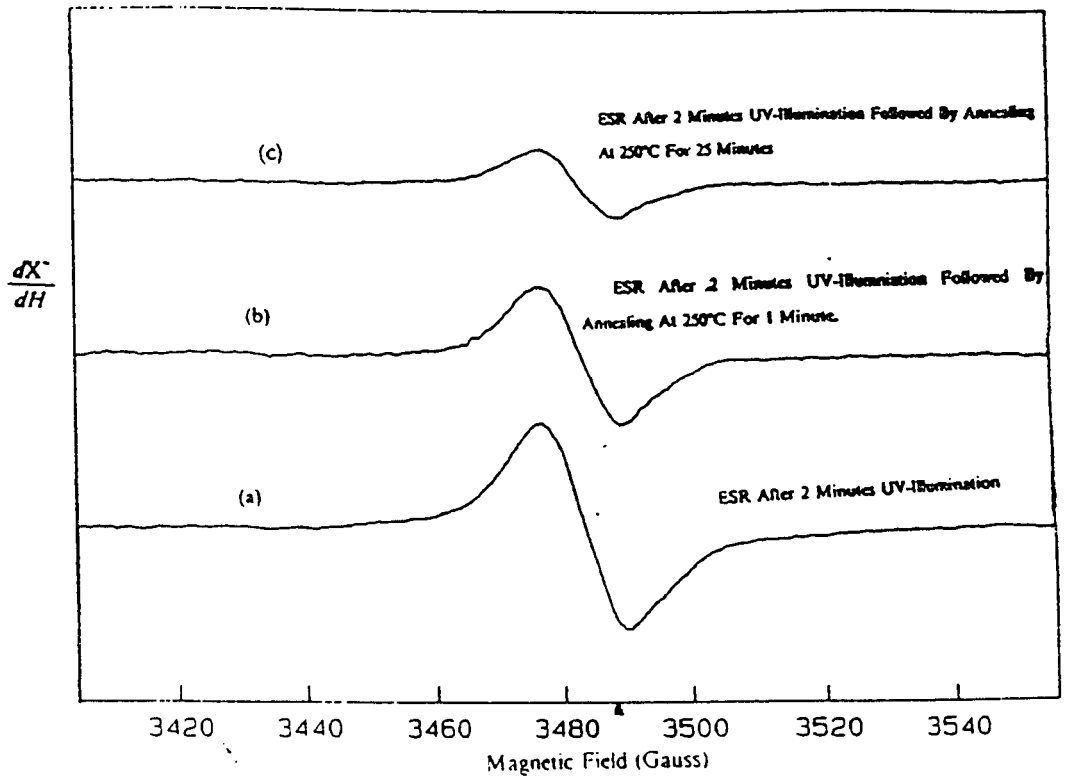
ESR After 2 Minutes UV-Illumination Followed By Annealing
At 250°C For 25 Minutes
(c)
ESR After 2 Minutes UV-Illumination Followed By
Annealing At 250°C For 1 Minute.
(b)
(a)
ESR After 2 Minutes UV-Illumination
dX/dH
3420
3440
3460
3480
3500
3520
3540
Magnetic Field (Gauss)

Annealing at room temperature (300K) was continued for about 1320 hours up to the level at which further annealing would result in no more decay of the light-induced ESR signal (saturation level). After about one hour of annealing a decay of 7% of the LESR is observed, while the total amount of decay due to the annealing at room temperature reached a maximum of 28% after 1320 hours. Study of the linewidth of the spectra is indicative of annealing the broader components of the LESR signal faster than the narrower components. A comparison between annealed signals of different time intervals of annealing at room temperature is shown in Fig 5.3. During the annealing a g value of 2.003 for the K_0 defects was detected. After annealing SiN at 300K to saturation, it is taken out of the cavity and reilluminated. The regenerated LESR signal is 99% of the initial LESR signal intensity. Annealing is a reversible phenomenon in a-SiN:H as long as the annealing temperature is limited to the deposition temperature used to prepare the thin film.

Annealing at 373K was carried out for 107 hours and the maximum decay detected at this temperature is about 61% of the LESR. Saturation annealing at 373K is achieved after 84 hours of annealing. No additional decay of the LESR is detected after 84 hours of annealing. To study the extent of reversibility of the light-induced defects, the sample is then re-illuminated with the UV lamp. In this study, annealing of the sample at 373K is found to be completely irreversible.

Figure 5.3

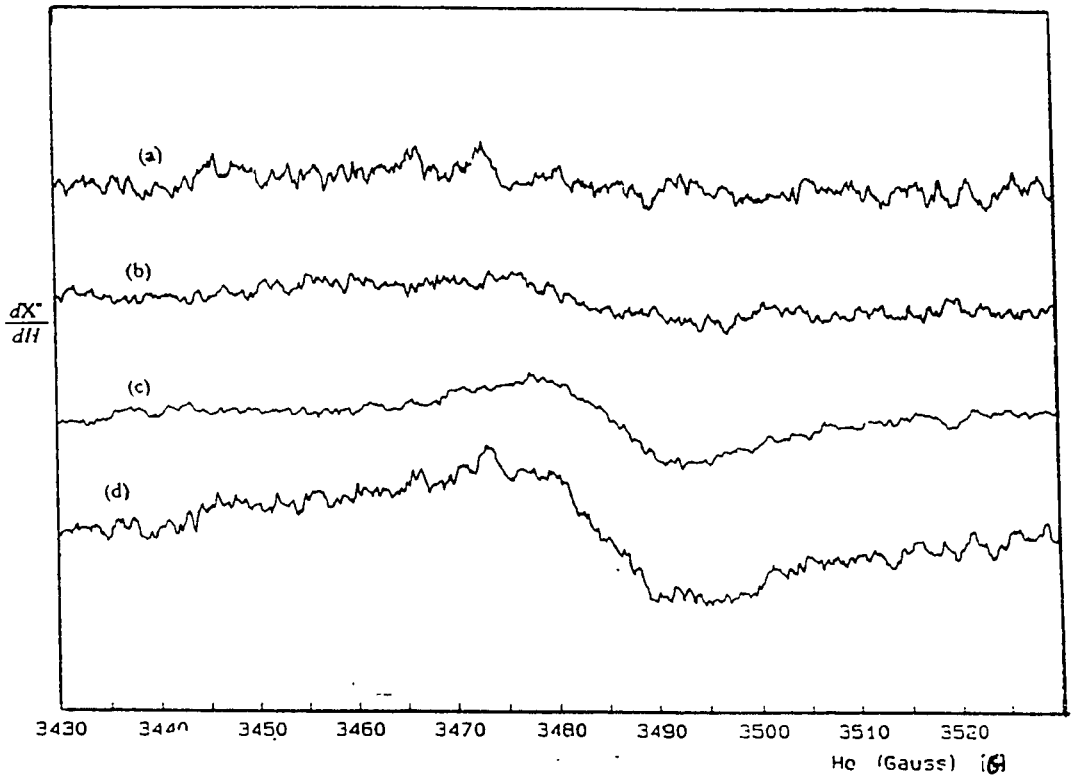

(a) (LESR Before Annealing) - (LESR Annealed At Room Temperature For 94 Seconds)

(b) (LESR Annealed At Room Temperature For 94 Seconds) - (LESR Annealed At Room Temperature For 1380 Seconds)

(c) (LESR Annealed At Room Temperature For 1380 Seconds) - (LESR Annealed At Room Temperature For 79153 Seconds)

(d) (LESR Before Annealing) - (LESR Annealed At Room Temperature For 79153 Seconds)

This result was unique for SiN samples and may be due to structural changes induced by prolonged heating.

A 423 K isothermal anneal was carried out for 2376 minutes. At this temperature, the saturation in the heat-induced decay of the LESR signal was found to be 58% of the LESR. To study the extent of the reversibility, this sample was reilluminated by UV-light for 2 minutes and 96% of the LESR signal was reproduced.

Annealing of the sample at 473K was carried out for 985 minutes. The sample was then left at room temperature for two days and further decay in the signal due to the annealing of the sample at room temperature was observed. The further decay in the LESR at room temperature shows that the sample was not annealed to saturation by heating the sample for 985 minutes. Therefore, annealing at 473 K was repeated. This time the annealing process was continued for 18 hours and 18 minutes until the saturation in the decay was observed . The total amount of decay in the LESR after 1099 minutes was 76% compared to the reference LESR signal. After the annealing process, the extent of reversibility was studied and almost 99% of the LESR was reproduced by reillumination of the sample. In Figure 5.43 the data recorded from both experiments at 473K is shown and the fitting curve parameters are compared in Table 5.1.

Figure 5.4

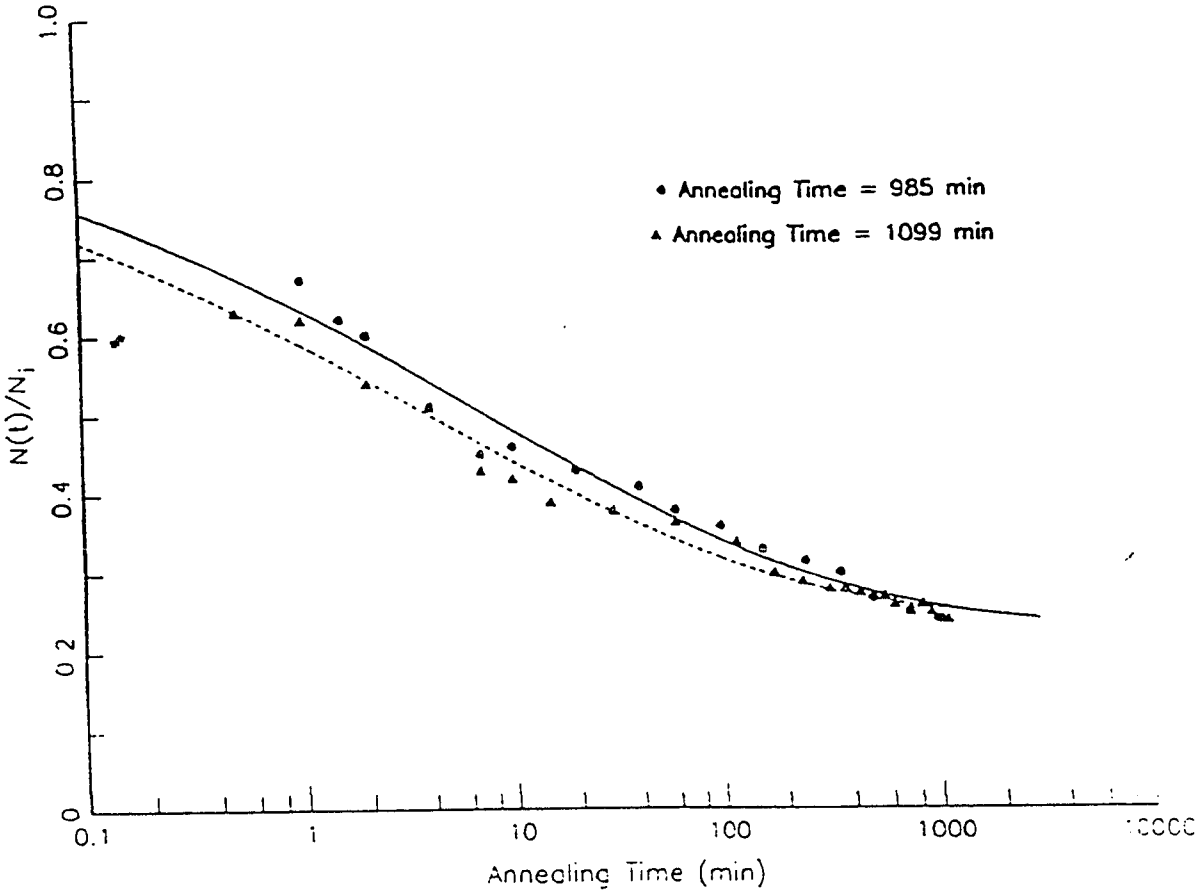
• Annealing Time = 985 min
▲ Annealing Time = 1099 min
N(t)/N$_i$
1.0
0.8
0.6
0.4
0 2
0
0.1
1
10
100
1000
Annealing Time (min)

Table 5.1

Annealing of LESR at 473 K			
Anneal time	A	β	τ (min)
985 (min)	77	.23	6
1099 (min)	76.4	.23	2.9

When the sample was annealed at 523K, the annealing process was carried out for 386 minutes. The signal taken at this point was even smaller than the "as deposited" signal (prior to the illumination), which is indicative of pre-existing LESR signals in this sample. Further, when this sample is left at room temperature for two days, additional decay in the ESR signal was observed. Thus, the annealing at 523 K was repeated. In another annealing experiment, prior to illumination, the sample was annealed at the same temperature that it was deposited (250 ° C) for about 2 hours and 30 minutes. This way about 40% of the as deposited defects in the sample were annealed out. Then the a-SiN:H film was illuminated until a maximum in the ESR signal was achieved. Annealing at 523 K was performed for 303 minutes and a saturation in the decay of LESR was observed within this period of time. After annealing, the reversibility of the production in light induced signal was detected . It was found that 77% of the LESR could be reproduced by reillumination of the sample.

To further detect the reversibility of annealing process the sample used for the first annealing experiment at 523 K was reilluminated for 2 minutes and 95% of the LESR was regenerated. This sample was reannealed for another 3 hours, and 85% decay in the reproduced LESR signal was observed. The sample was reilluminated for 45 seconds and again 95% of the reference LESR was regenerated. At this stage, the

sample was further illuminated for another 10 seconds and a small amount of annihilation of the ESR was observed .

In Fig. 5.5 the data from both experiments done at 523 K is shown, and the fitting parameters are compared in Table 5.2. Thus, it appears that annealing at 523K will produce some irreversible changes in the cycling of the LESR signal while lower annealing temperature produce only reversible changes.

The time dependent decay of the LESR signal in a-SiN:H during isothermal annealing in different temperatures as a function of time is shown in Fig. 5.6. The stretched exponential function (eq. 5.2) was used to best fit the isothermal annealing curves. The parameters A, β, and τ are found by curve fitting (eq.5.2) with the data and are shown in Table 5.3.

The τ versus annealing temperature is shown in Fig. 5.7. By fitting the Arrhenius relation (see eq. 5.3), the data values for τ_0 and E_a is found to be 1.46×10^{-2} sec. and 0.425 eV, respectively.

Figure 5.5

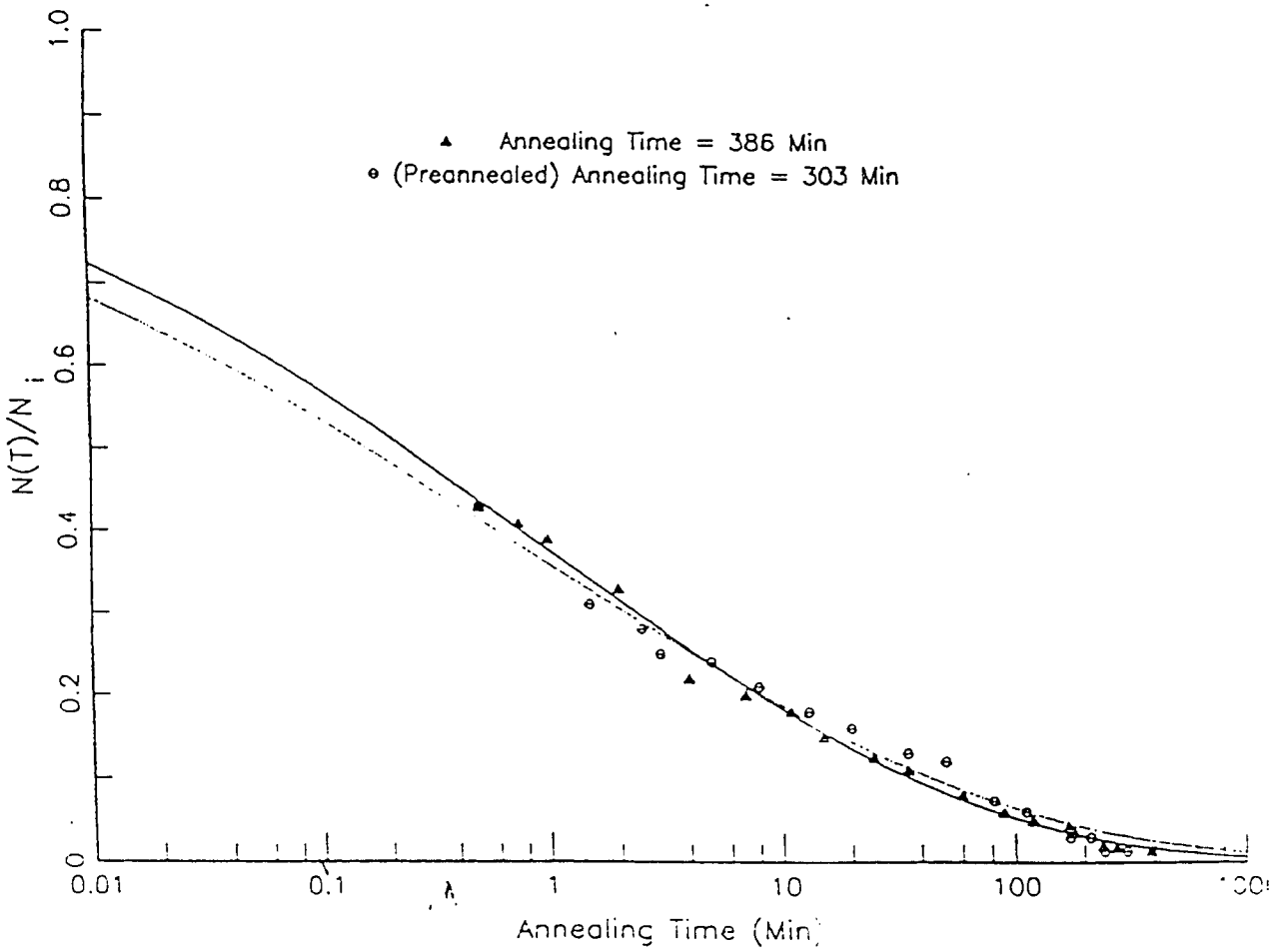
▲ Annealing Time = 386 Min
⊖ (Preannealed) Annealing Time = 303 Min
N(T)/N i
1.0
0.8
0.6
0.4
0.2
0
0.01
0.1
1
10
100
Annealing Time (Min)

Table 5.2

Annealing of LESR at 523 K			
Anneal time	A	β	τ (min)
303 (min)	100	.21	.9
386 (min)	100	.24	1.1

Figure 5.6

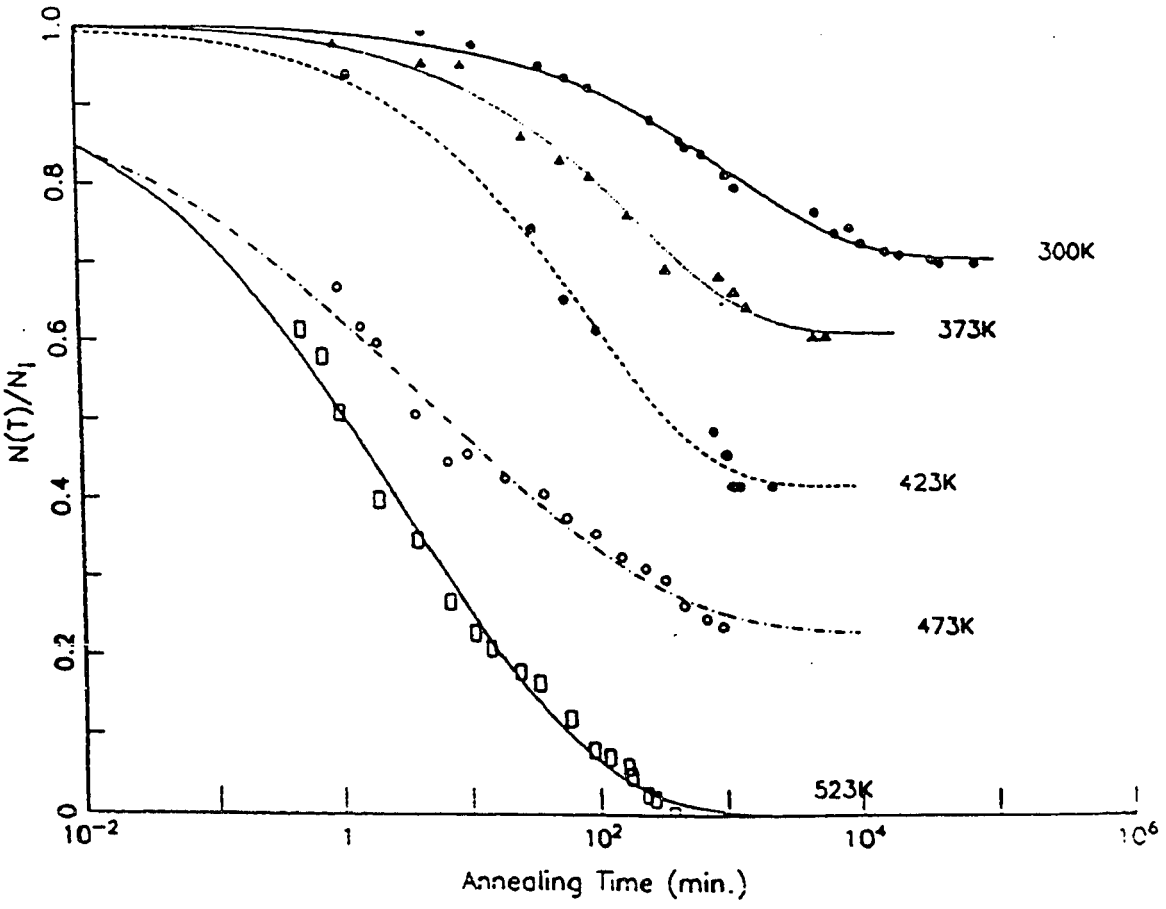
1.0
0.8
0.6
0.4
0.2
0
N(T)/N_i
300K
373K
423K
473K
523K
10^-2
1
10^2
10^4
10^6
Annealing Time (min.)

Table 5.3

Annealing of LESR data			
Temp. (K)	A	β	τ (min)
300	29	.49	1509
373	38	.49	260
423	58	.45	95
473	77	.23	2.9
523	100	.22	1.1

Figure 5.7

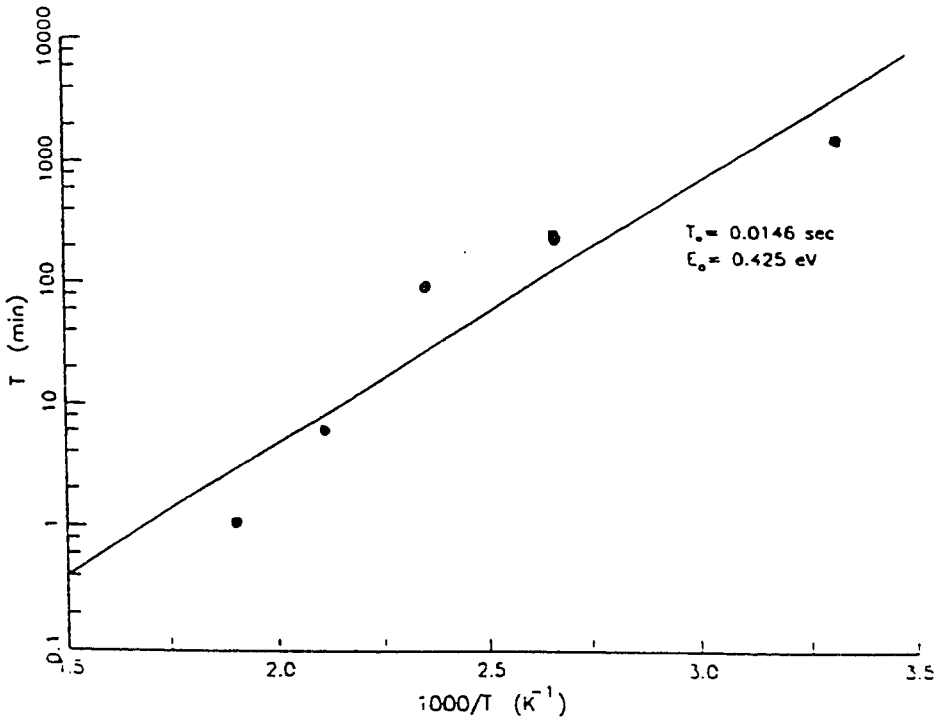
τ (min)
10000
1000
100
10
1
0.1
1.5
2.0
2.5
3.0
3.5
1000/T (K⁻¹)
τ₀= 0.0146 sec
E₀= 0.425 eV

5.2 Discussion

Comparing the changes in the LESR signal due to isothermal annealing and annihilation processes, we can predict that the mechanism involved in isothermal annealing is different from that for the annihilation process. To provide an explanation for thermal annealing of light-induced K^0 centers in SiN we detect changes of β with respect to the changes of temperature. During isothermal annealing of LESR below 473 ° K, β is independent of temperature (Fig. 5.8). A temperature-independent β represents tunneling or hopping mechanism [5.5-5.7]. In this case the dispersion is due to the distribution of the wave functions at localized states.

However, when the annealing temperature is above 473 ° K, a decrease in the β value is observed. This decay in β may indicate that the deep traps in the midgap are activated by heating the sample above 473 ° K. Therefore more K^0 centers are available to trap electrons, as well as more K^- centers are available to release electrons.

The observed behavior at temperatures above 473 ° K can also indicate that, in addition to the hopping process, local structural changes are occurring during the annealing process. For example, hydrogen released

from a N-H bond can passivate a local silicon dangling bond and consequently decrease the LESR signal. These local structural changes can be reversed by reilluminating the sample with the UV light.

Figure 5.8

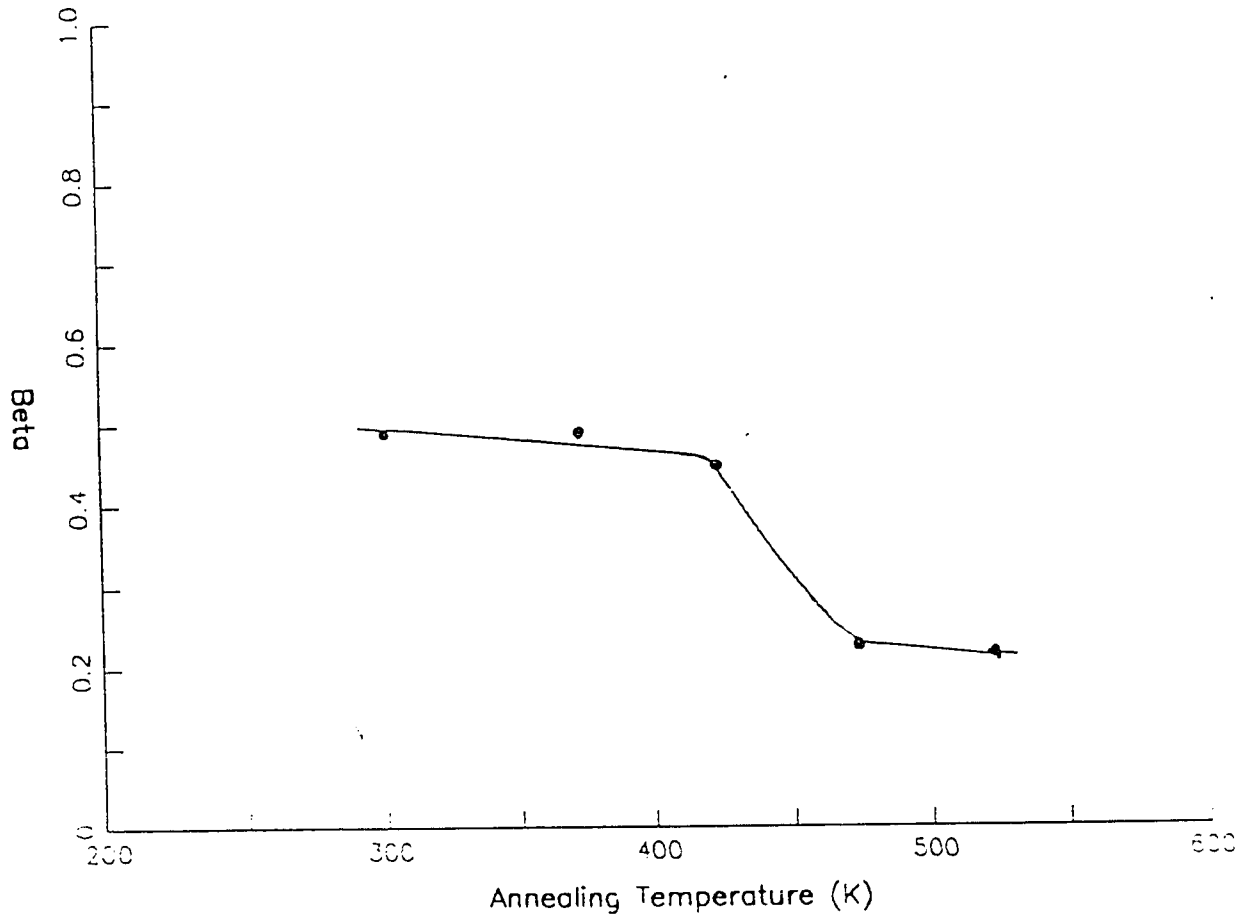

The hopping mechanism is a phonon-assisted quantum mechanical tunneling of an electron from one localized state to another localized state. Considering negative correlation energy (4.15) for the localized states, one of the possible tunneling processes can be two electrons from a K^- state located below the Fermi energy sent into two different K^0 states nearby, changing them to two new K^- states. The energy separation of initial and final states is denoted by the energy barrier . Due to the conservation energy, a phonon should be absorbed or emitted during the hopping process for passing the energy barrier. This makes the hopping process finite at finite temperatures. However, the number of the phonon states increases by increasing the temperature, and consequently, it will be more favorable for the electron to pass larger energy barriers and make a longer hop. This way, by increasing temperature, more K^0 centers can trap electron or holes. In our model the thermal activation energy is about 0.4 eV, which represents the energy barrier for the hopping process in the midgap. Therefore, the carriers can hop with a constant hopping energy (0.4 eV) between the states in the gap. However, by annealing the sample at higher temperature, the carriers can pass higher energy barrier and consequently causes a strong dispersion. This can also be another explanation for our observation in the annealing the samples above 473 ° K.

To determine the reversibility of the annealing mechanism, after annealing the samples at different temperatures, each sample was reilluminated by UV light and a high degree of restoration of the LESR signal ($\sim$ 90%) was observed. This result is a good evidence of tunneling and hopping processes involved in the annealing process. However, a small amount ($\sim$ 10%) of LESR could not be reproduced by reillumination of samples, which suggests that a structural change is occurring by the annealing process. This structural change can be due to the hydrogen diffusion in the sample and can be increased by increasing the annealing time.

6. Summary

Short time UV-exposure can populate neutral defects in the amorphous silicon nitride produced at 250 ° C, which can be irreversibly annihilated by longer UV-illumination. The light-induced defects can be annealed by heating the sample at temperatures between 300 to 523 ° K and can be reproduced by reillumination of the sample for a short time. The reversible changes can arise from the charge motion or local structural changes, where the irreversible changes can be due to the structural changes. Comparing the SiN films used in this study with the films produced at 400 ° C , we find more hydrogen in these films which apparently contributes to our results.

Two different models are suggested for the annihilation mechanism. One model involves the hydrogen motion and configuration rearrangement, where the other model is due to the charge motion between the K^0 centers. The IR study performed on the annihilated sample has shown that under long time UV- exposure the concentration of the N-H bond decreases and the concentration of the Si-H bond increases. Therefore, one possible mechanism for the annihilation of the LESR signal is through the rearrangement of the bond configuration and consequently breaking

N-H bonds where the produced hydrogen bonds can diffuse through the sample and passivate the light- induced silicon dangling bonds. Another possible mechanism due to the configuration rearrangement is breaking the H-H bond and diffusing the hydrogen through the sample and passivating the Si dangling bond.

Good evidence for the contribution of hydrogen diffusion in the results observed at room temperature is the broadening of the ESR signal caused by the hyperfine interaction between the magnetic moment of the unpaired electron of the silicon with the magnetic moment of the hydrogen nucleus. Low temperature study shows a small amount of annihilation which is more good evidence for the contribution of hydrogen to our results. The observed decay at low temperature may be an artifact due to the fact that we are detecting the LESR signal at room temperature.

Another model suggested for the annihilation process is due to the charge motion. In this model the K^0 centers can act as the trapping centers for the photo-excited electrons and holes which results in the stable diamagnetic charged trapping centers. This model is consistent with the electrical stress measurement which shows that even though a large number of the K^0 centers are annihilated , the number of the trap centers remain almost unaffected.

The stretched exponential annealing kinetics for the light-induced K^0 centers is indicative of a dispersive annealing process such as hopping, multiple trapping, or trap controlled hopping. Isothermal annealing of LESR in this study shows a temperature independent β, which represents tunneling or hopping transport mechanisms. In this case, the dispersion is due to a distribution of the wave functions of the localized states.

When the sample is annealed above 473 ° K, a decrease in the β value is observed. This result is unusual and may indicate that the deep traps in the midgap are activated by heating the sample above 473 °K and consequently more K^0 centers are available to trap electrons, as well as more K^- centers are available to release electrons. The observed behavior at temperatures above 473° K may more likely be due to the local structural changes that are reversible by reilluminating the sample with the UV-light. The thermal activation energy in our study is about 0.4 eV, which represents the energy barrier for the hopping process in the mid gap.

Annealing study shows that the annealing process is highly reversible and it requires an annealing temperature equal to or greater than that of the deposition temperature to completely depopulate all of the light-induced K^0 centers from the film.

7. References

1.1 P.G. Lecomber and W.E. Spear, *In Semiconductors And Semimetals* , Vol.2 , D, (1984)

1.2 T.L. Chu, J.R. Szedon, and C.H. Lee, Solid State Electron ***10*** , 897 (1967)

1.3 V.G. Krasov, Obzory Po Elektron. Ser. 6, Vol. 6 (1978)

1.4 V.I Belyl, L.L. Vasilyeva, A.S. Ginovker, V.A. Gritsenko, S.M. Repinsky, S.P. Sinitsa, T.P. Smirnova, F.L. Edelman, *Silicon Nitride In Electronics* , Elsevier, NY, (1988)

1.5 K.L. Ngal and Hsia Y., Appl. Phys. Lett. ***41*** 159 (1982)

1.6 J. Robertson and M.J. Powell, J. Appl. Phys. ***44*** ,415(1986)

1.7 K.L. Ngia and Y. Hsia, Appl. Phys. Lett. ***41*** , 159 (1982)

1.8 S.T. Pantelides, Phys. Rev. ***B57*** , 2979 (1986)

1.9 D.T. Krick, P.M. Lenahan and J. Kanicki, J. Appl. Phys. ***64*** 3558 (1988)

1.10 D.L. Staebler and C.R. Wronski, J. Appl. Phys. ***51*** , 3262 (1980)

1.11 E. Tober, M.S. Thesis, San Jose State Univ., (1990)

1.12 H.Dersch, J. Stuke, and J. Beichler, Appl. Phys. Lett. ***38*** , 456 (1980)

1.13 S. Yokoyama, M. Hirose, and Y. Osaka, Jpn. J. Appl. Phys. ***20*** , 35 (1980)

1.14 T. Makino and M Maeda, Jpn. J. Appl. Phys. *25* , 1300 (1986)

1.15 M. Kumeda, H. Yokomichi, T. Shimizu, Jpn. J. Appl. Phys. *23* ,502 (1984)

1.16 D. Jousse, J. Kanicki, D.T. Krick, and P.M. Lenahan, Appl. Phys. Lett. **52** , 445 (1988)

1.17 Yokoyama, M. Hirose, and Y. Osaka, Jpn. J. Appl. Phys. **20** , L35 (1980)

2.1 A. Carrington and A.D. McLachlan, *Introduction To Magnetic Resonance* , Harper and Row, NY, London (1967)

2.2 C.P. Poole, *Electron Spin Resonance* 2nd Ed., Wieley- Interscience, NY, NY, (1983)

2.3 G.E. Pake and T.L. Estle, *The Physical Principles Of Electron Paramagnetic Resonance* , W.A. Benjamin Inc., Mass. (1973)

3.1 M.H. Brodsky, *Amorphous Semiconductors*, Springer- Verlag, N.Y., N.Y., (1985)

3.2 R. Zallen, *The Physics Of Amorphous Solids, Wiley-Interscience* , N.Y., N.Y., (1983)

3.3 M.H. Cohen, H. Fritzche, S.R. Ovshinsky, Phys. Rev. Lett., **22** , 1065 (1969)

3.4 Michael Pollak, *Noncrystalline Semiconductors* , CRC, Vol.1, (1987)

3.5 B. Von Roedern, L. Ley, M. Cardona, Phys. Rev. Lett., **39** , 1576, (1977)

3.6 J. Robertson, Philosophical magazine, B, Vol.63, No.1, 47-77, (1991)

3.7 R.A. Street, Adv. Phys. Lett. **25** , 397, (1976)

3.8 S.G. Bishop, U. Strom, and P.C. Taylor, Phys. Rev. Lett. **36** 543 (1976)

3.9 D. Vanderbitt, Phys. Rev. lett. **49** , 823, (1982)

3.10 D. Alder, J. Non-Crystall. Solids, **42** 315-334, (1980)

3.11 D.L. Staebler and C.R. Wronski, Appl. Phys. Lett. *31* 292 (1977)

3.12 M. Kumeda, H. Yokomichi, T. Shimizu, Jpn. J. Appl. Phys. *23* , 502 (1984)

3.13 H. Yokomichi, M. Kumeda, A. Morimoto, and Shimizu, Jpn. J. Appl. Plys. *24* , 569 (1985)

3.14 M.S. Crowder, E.D. Tober, and J. Kanicki, Appl. Phys. Lett. *57* , 1995 (1990)

3.15 N.R.J. Poolton and Y. Cros, J. Phys. I *1* France, 1335-1345, (1991)

3.16 J.L. Pankove, J.E. Berkeyheiser, Appl. Phys. Lett. *37* , 705.

3.17 D. Alder, M.E. Eberhart, K.H. Johnson, and S.A. Zygmunt, J. Non. Crys. Sol. *66* , 273, (1984)

5.1 D.T. Krick, P.M. Lenahan, and J. Kanicki, Appl. phys. Lett. *51* , 608, (1987)

5.2 H. scher and E.W. Montron, Phys. Rev. *12* , 2455 (1975)

5.3 E. Tober, J. Kanicki, and M.S. Crowder, Appl. Phys. Lett. *59* , 1723 (1991)

5.4 W.E. Jackson, J. Kakalios, Phys. Rev. *B37* , 1020 (1988)

5.5 P. Nagels, *Amourphous Semiconductors* , M.H. Brodsky N.Y. (1985),

P. 136

5.6 G. Pfister and H. Scher, Phys. Rev. ***B15***, 2062 (1977)

5.7 D.T. Krick, P.M. Lenahan, and J. Kanacki, Appl. Surf. Sci. ***39*** , 392, (1989)

8. Figure Captions

Figure 1.1 Schematic representation of defect as: a) a monovacancy in the crystalline, b) a dangling bond in the amorphous (b).

Figure 2.1 Zeeman split electron spin level in a magnetic field.

Figure 2.2 Zeeman split electron spin level in a magnetic field for a system with S = 1/2 and I = 1.

Figure 3.1 Density of states vs. energy for amorphous semiconductors with defect states in the midgap.

Figure 3.2 Energy level diagram for states in the gap of amorphous silicon.

Figure 3.3 Two level energy well system vs. configuration coordinate K, for the ground state and metastable states.

Figure 3.4 ESR traces of amorphous silicon nitride film a) as deposited film (DESR), b) after annealing the film for 300 minutes magnified 3 times.

Figure 4.1 Photo-production and annihilation of LESR vs. illumination time for "as received" sample.

Figure 4.2 ESR traces, a) after 2 minutes illumination with UV-light b) after 1104 minutes illumination with UV-light magnified 4 times.

Figure 4.3 ESR traces of hydrogenated amorphous silicon a) after 2 minutes broadband illumination b) after 30 minutes broadband illumination c) after 1101 minutes broadband illumination.

Figure 4.4 Photo-production and annihilation of LESR vs. illumination time for the preannealed sample.

Figure 4.5 Photo-production and annihilation of LESR vs. illumination time: (●) illumination at 77K, (▲) illumination at room temperature, (□) reillumination at 77K.

Figure 5.1 ESR traces of hydrogenated amorphous silicon film a) after 2 minutes broadband illumination, b) after 2 minutes UV-illumination followed by annealing at 250° C for 25 minutes magnified 3.3 times.

Figure 5.2 ESR traces of hydrogenated amorphous silicon film, a) after 2 minutes UV-illumination, b) after 2 minutes UV-illumination followed by annealing at 250°C for 1 minute, c) after 2 minutes UV-illumination followed by annealing at 250°C for 25 minutes.

Figure 5.3 LESR traces of hydrogenated amorphous silicon film at room temperature: a) (LESR before annealing) - (LESR annealed for 94 seconds), b) (LESR annealed for 94 seconds) - (LESR annealed for 1380 seconds), c) (LESR annealed for 1380 seconds) - (LESR annealed for 79153 seconds), d) (LESR before annealing) - (LESR annealed for 79153 seconds).

Figure 5.4 Isothermal annealing of the normalized LESR signal intensity at 200° C vs. annealing time: a) (•) total annealing time: is 985 minutes, b) (▲) total annealing time is 1099 minutes.

Figure 5.5 Isothermal annealing of the normalized LESR signal intensity at 250 ° C: a) (▲) annealing of LESR for 386 minutes, b) (⊖) annealing of LESR for 303 minutes in the preannealed film.

Figure 5.6 Isothermal decay of the normalized LESR signal intensity vs. annealing time for annealing temperatures ranging from 298 K to 523

K. The data is least-squares fit with the stretched exponential equation $A \exp[-(\frac{t}{\tau})^{\beta}] + (1 - A)$.

Figure 5.7 τ vs. inverse annealing temperature. The data is fit with the Arrhenius relation $\tau = \tau_0 \exp(\frac{E}{<k_b} T)$.

Figure 5.8 Fitting parameter β vs annealing temperature. The data is fit with the equation $\beta = \frac{T_A}{T_0}$.